ORNL/TM-7674

ornl

OAK RIDGE NATIONAL LABORATORY

UNION CARBIDE

Performance of HTGR Biso- and Triso-Coated Fertile Particles Irradiated in Capsule HT-34

E. L. Long, Jr.
T. N. Tiegs
J M Robbins
M. J. Kania

METALS and CERAMICS
ENERGY
RESEARCH
DEVELOPMENT
OAK RIDGE NATIONAL LABORATORY

OPERATED BY
UNION CARBIDE CORPORATION
FOR THE UNITED STATES
DEPARTMENT OF ENERGY

ORNL/TM-7674
Distribution
Category UC-77

Contract No. W-7405-eng-26

METALS AND CERAMICS DIVISION

HTGR BASE TECHNOLOGY PROGRAM

Fuel Graphite Development (FTP/A 01330)

PERFORMANCE OF HTGR BISO- AND TRISO-COATED FERTILE PARTICLES IRRADIATED IN CAPSULE HT-34

E. L. Long, Jr., T. N. Tiegs, J M Robbins, and M. J. Kania

Date Published: August 1981

OAK RIDGE NATIONAL LABORATORY
Oak Ridge, Tennessee 37830
operated by
UNION CARBIDE CORPORATION
for the
DEPARTMENT OF ENERGY

CONTENTS

PERFORMANCE OF HTGR BISO- AND TRISO-COATED FERTILE PARTICLES IRRADIATED IN CAPSULE HT-34

E. L. Long, Jr., T. N. Tiegs, J M Robbins, and M. J. Kania

ABSTRACT

Experiment HT-34, irradiated in the target region of the High Flux Isotope Reactor (HFIR), was designed to correlate HTGR Biso- and Triso-coated particle performance with fabrication parameters. Gamma analysis of the irradiated Triso-coated ThO_2 particles showed that the SiC deposited at the highest coating rate apparently had the best cesium-retention properties. Results of a similar analysis of the irradiated Biso-coated ThO_2 particles showed no differences in performance that could be related to coating conditions, but all the particles showed a significant loss of cesium (>50%) at the higher temperatures. Pressure-vessel failures occurred with a significant number of particles; however, fission-gas-content measurements made at room temperature showed that the intact Biso particles from all batches except one became permeable during irradiation. Partial or complete loss of fission gas from a few particles in a sample implied that significant coating-property variations exist within any given batch. A possible source of uncertainty in interpreting the permeability results may have been introduced because the Biso particles prepared in the large coater received no postcoating anneal. Biso particles from a batch prepared in the small coater with a CO_2 diluent showed outstanding performance in earlier experiments but were found to become permeable during irradiation in HT-34. In contrast, inert-gas-intrusion measurements on Biso-coated inert (carbon) particles showed, without exception, a marked decrease in permeability.

INTRODUCTION

The HT-34 experiment, irradiated in the target region of HFIR, was a cooperative effort between General Atomic Company (GA) and Oak Ridge National Laboratory (ORNL), with about one-half the irradiation space allocated to each. The GA Triso-coated ThO_2 test specimens were irradiated in the upper portion of the capsule in loose-particle holders. The ORNL Triso- and Biso-coated ThO_2 test specimens were irradiated in the lower portion of the capsule in bonded-bed specimens and loose-particle holders, respectively. The GA results will be reported separately;[1] therefore, they will not be discussed in this report.

The detailed objectives for the ORNL test specimens were:

1. To investigate the influence that differences in pyrocarbon microstructures, which result from variations in fabrication process conditions, had on a coating's ability to retain fission gases and remain resistant to fast-neutron damage. Specific process variables thought to influence Biso-particle irradiation performance are hydrocarbon coating gas, deposition temperature, diluent type, and diluent concentration. Process variables were systematically varied as outlined in Fig. 1. Coating properties of interest include pyrocarbon coating rate, density, anisotropy, and permeability. Optimization of the process variables listed here will provide guidelines for operation of the 0.24-m coating furnace.

2. To evaluate the performance of SiC layers of Triso-coated ThO_2 particles deposited at higher coating rates (about 0.5 μm/min) than those previously employed (about 0.2 μm/min). The fuel product specification for the Triso-coated particle requires that 99% of the SiC coatings have a density exceeding 3.18 Mg/m^3. To meet this requirement, the SiC layer was deposited at very low deposition rates — 0.1 to 0.2 μm/min — to ensure integrity of the coating. From an economic standpoint, SiC coatings deposited at higher coating rates without loss of coating integrity would be more desirable. Specific performance characteristics investigated were the fission product retention, the coating's mechanical integrity, and the influence of the SiC microstructure on these performance aspects.

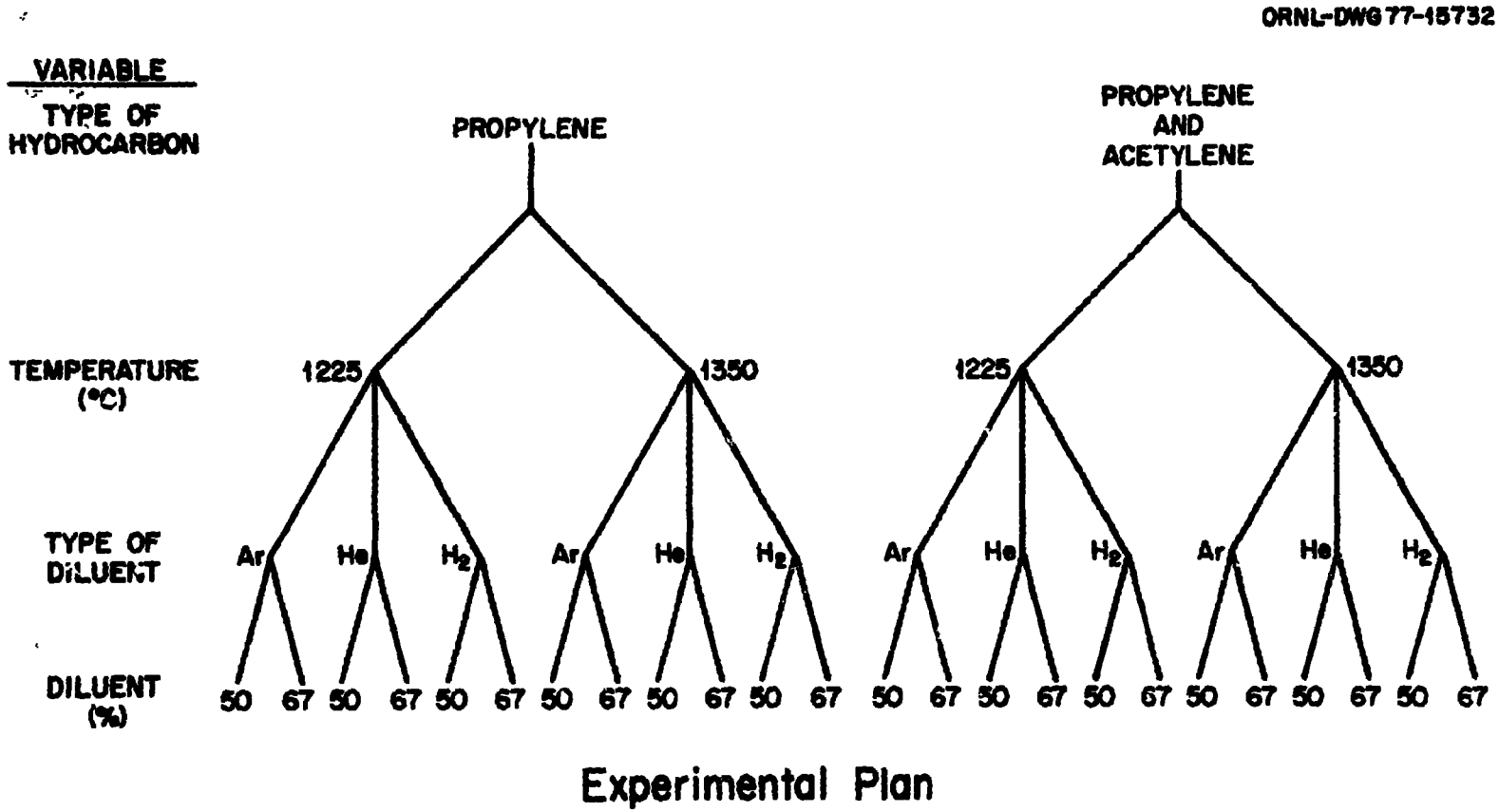

Fig. 1. Process Variables and Respective Ranges Used in Experiment HT-34 to Study the Influence on Overall Performance of Biso-coated ThO_2 Particles.

3. To correlate permeability measurements made with light inert gases and those made with fission-gas release-to-birth (R/B) ratios. Current design criteria restrict fission-gas R/B ratios for the isotope ^{85m}Kr to less than 3×10^{-5} at 1100°C for irradiated particles. There is control procedure currently available for measuring and predicting fission-gas release on unirradiated particles. However, a technique has been developed at ORNL to correlate measurements of pyrocarbon permeability to light inert gases on unirradiated particles with pyrocarbon permeability to fission gases after irradiation. Particle batches from objective 1 were also used to meet this objective.

4. To resolve irradiation performance anomalies between two similar particle designs, batch OR-1975-T and batch OR-2013-T, which were irradiated in HFIR target capsules HT-18 and -19. The only difference in the fabrication of these two Biso ThO_2 particle batches was that batch OR-2013-T had a low-temperature isotropic (LTI) coating deposited from a carrier gas of CO_2 + argon instead of just argon. Batch OR-1975-T was of the reference fertile design and was expected to survive all temperatures and fluences in the series. Consequently, it was irradiated in HT-19 only, in the high-temperature, high-fluence region. Instead of complete survival, the particles showed greater than 90% failure. Batch OR-2013-T, with the fabrication difference we have stated, was irradiated in the capsule positions in HT-18 and -19 that received the highest fluence and experienced the peak operating temperatures. Interestingly, this particle survived completely in both capsules. To resolve the anomaly, particles from both batches were irradiated in a specially designed holder so that both particle types received the same neutron fluence and experienced the same operating temperatures. Additionally, two batches of carbon kernels with Biso coatings that duplicated the coating designs of the two batches of ThO_2 particles were irradiated in the magazine end caps.

CAPSULE DESIGN

As indicated earlier, capsule HT-34 was shared between GA and ORNL; the capsule design is shown in Fig. 2. The upper half of the capsule

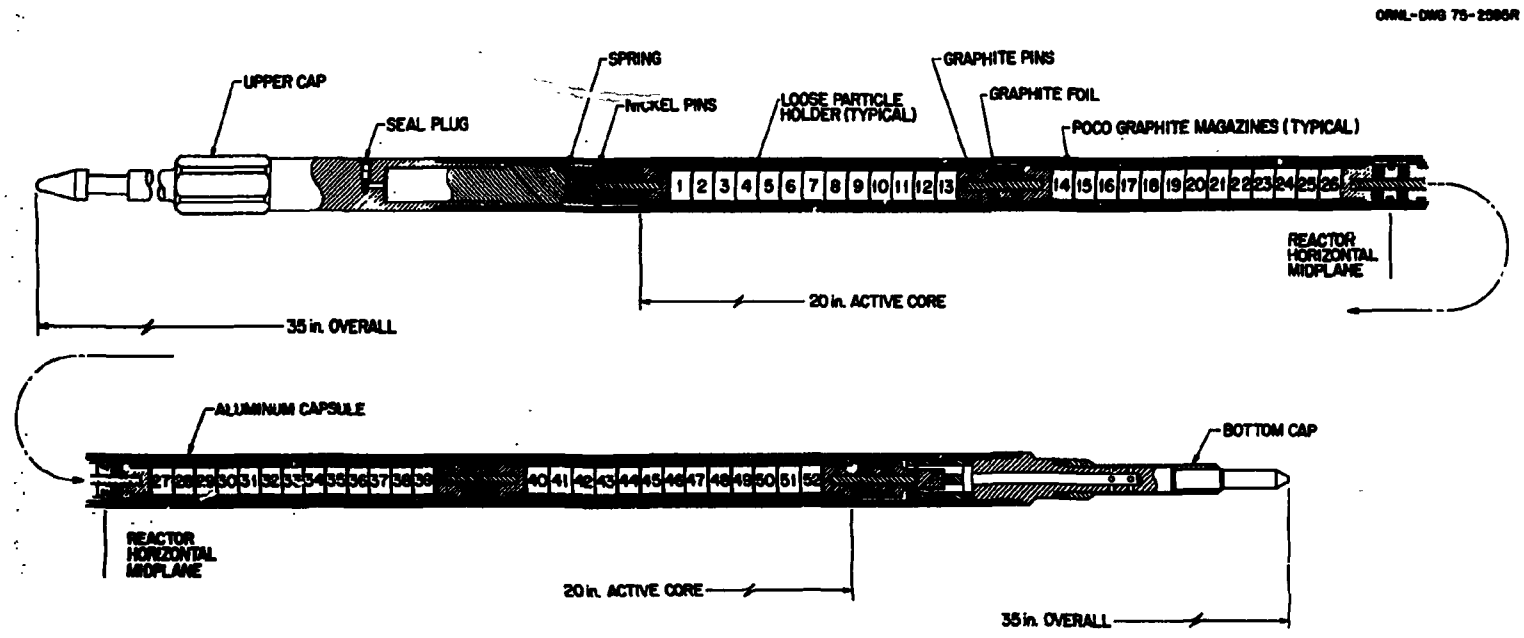

Fig. 2. The HT-34 Capsule Design (1 in. = 25.4 mm).

contained the GA test specimens. The driver particles (uranium with 7%-enriched ^{235}U) were contained in warm-molded bonded-bed specimens. Triso-coated ThO_2 test particles were placed in loose-particle holders. Heavy metal loadings were such that operating temperatures (maximum particle surface temperature) would be about 1250°C in the low-temperature region and about 1550°C in the high-temperature region. Specimen placement and heavy metal loadings for capsule HT-34 are described in Tables 1 and 2, respectively.

The lower half of the capsule contained ORNL test specimens. This portion was redesigned to provide irradiation temperatures of 1250°C in the high-temperature region and 900°C in the low-temperature region. Important design changes were new magazine dimensions and a reduced heavy metal loading for each irradiation position (specimen placement and heavy metal loadings are described in Tables 1 and 2, respectively). Fuel specimens were Biso- and Triso-coated ThO_2 particles. The Biso particles were irradiated in loose-particle holders, and the Triso particles were irradiated along with the driver particles in warm-molded bonded-bed specimens. The fill gas used in this capsule was argon.

PREPARATION OF TEST SPECIMENS

Eight batches of Biso-coated ThO_2 particles were prepared in the 0.13-m coating furnace, using the fritted gas distribution system to meet objectives 1 and 3 (ref. 2). A systematic variation of the fabrication process variables, as outlined in Fig. 1, was employed. The specific ranges were chosen so that limits of successful performance could be obtained for each process variable. Maximum characterization of all coating properties thought to influence overall performance was obtained. The eight batches were selected because they had acceptable LTI thickness and densities, the highest quality particles in terms of BAF_0 and Ne/He ratio, and the lowest fraction defective as determined by 1000°C gaseous chlorine leach and fission-gas R/B ratios. All pertinent characterization data for these eight Biso particle batches are shown in Table 3. As a part of objective 3, inert Biso-coated particles from three batches produced in small laboratory coaters were included to allow for a comparison of pre- and post-irradiation permeability measurements (Table 3).

Table 1. Loading Scheme for Irradiation Capsule HT-34

Position[a]	Temperature (°C)	Specimen Type	Fuel (Heavy Metal)	Batch[b]	Coating Type
End plug 14-3	1250	Loose	Th	7032-149	Triso
1	1250	Bonded	U	OR-2576-H	Triso
2	1250	Loose	Th	-20-0161-001	Triso
3	1250	Bonded	U	OR-2576-H	Triso
4	1250	Loose	Th	-07-0262	Triso
5	1250	Loose	Th	-14-0261-001	Triso
6	1250	Bonded	U	OR-2576-H	Triso
7	1250	Loose	Th	-14-0171-001	Triso
8	1250	Loose	Th	-13-0161-002	Triso
9	1250	Bonded	U	OR-2576-H	Triso
10	1250	Loose	Th	-14-0161-001	Triso
11	1250	Loose	Th	-15-0161-001	Triso
12	1250	Bonded	U	OR-2576-H	Triso
13	1250	Loose	Th	-16-0161-001	Triso
End plug 14-1	1250	Loose	Th, inerts	7032-149, 6351-04-0100	Biso/Triso[c]
End plug 15-3	1550	Loose	Th	7032-149	Triso
14	1550	Bonded	U	OR-2576-H	Triso
15	1550	Loose	Th	-20-0161-002	Triso
16	1550	Bonded	U	OR-2576-H	Triso

Table 1 (Continued)

Position[a]	Temperature (°C)	Specimen Type	Fuel (Heavy Metal)	Batch[b]	Coating Type
17	1550	Loose	Th	-07-0262-002	Triso
18	1550	Loose	Th	-14-0161-002	Triso
19	1550	Bonded	U	OR-2576-H	Triso
20	1550	Loose	Th	-14-0271-001	Triso
21	1550	Loose	Th	-14-0181-001	Triso
22	1550	Bonded	U	OR-2576-H	Triso
23	1550	Loose	Th	-17-0161-001	Triso
24	1550	Loose	Th	-15-0171-001	Triso
25	1550	Bonded	U	OR-2576-H	Triso
26	1550	Loose	Th	-13-0171-001	Triso
End plug 15-1 RHMP[d]	1550	Loose	Th, inerts	7032-149, 6351-04-0100	Biso/Triso[c]
End plug 26-1	1250	Loose	Inert	OR-2730-1	Biso
27	1250	Loose	Th	A-765	Biso
28	1250	Bonded	Th, U	A-834, OR-2576-H	Triso/Triso
29	1250	Loose	Th	A-780	Biso
30	1250	Loose	Th	A-785	Biso
31	1250	Bonded	Th, U	A-835, OR-2576-H	Triso/Triso
32	1250	Loose	Th	A-806	Biso

Table 1 (Continued)

Position[a]	Temperature (°C)	Specimen Type	Fuel (Heavy Metal)	Batch[b]	Coating Type
33	1250	Loose	Th	A-762	Biso
34	1250	Bonded	Th, U	A-837, OR-2576-H	Triso/Triso
35	1250	Loose	Th	A-782	Biso
36	1250	Loose	Th	A-786	Biso
37	1250	Bonded	Th, U	A-836, OR-2576-H	Triso/Triso
38	1250	Loose	Th	A-787	Biso
39	1250	Loose	Th	OR-1975-T, OR-2013-T	Biso
End plug 26-3	1250	Loose	Inert	OR-2722-1, OR-2725-1	Biso
End plug 28-1	900	Loose	Inert	OR-2730-1	Biso
40	900	Loose	Th	A-765	Biso
41	900	Bonded	Th, U	A-834, OR-2576-H	Triso/Triso
42	900	Loose	Th	A-780	Biso
43	900	Loose	Th	A-785	Biso
44	900	Bonded	Th, U	A-835, OR-2576-H	Triso/Triso
45	900	Loose	Th	A-806	Biso
46	900	Loose	Th	A-762	Biso
47	900	Bonded	Th, U	A-837, OR-2576-H	Triso/Triso
48	900	Loose	Th	A-782	Biso
49	900	Loose	Th	A-786	Biso

Table 1 (Continued)

Position[a]	Temperature (°C)	Specimen Type	Fuel (Heavy Metal)	Batch[b]	Coating Type
50	900	Bonded	Th, U	A-836, OR-2576-H	Triso/Triso
51	900	Loose	Th	A-787	Biso
52	900	Loose	Th	OR-1975-T	Biso
End plug 28-3	900	Loose	Inert	OR-2722-1, OR-2725-1	Biso

[a] From top of capsule.

[b] Loose ThO_2 particles preceded by "6252-" unless noted otherwise.

[c] LTI burned off.

[d] Reactor horizontal midplane.

Table 2. Heavy Metal Loadings for Irradiation Capsule HT-34

Position[a]	Design Temperature (°C)	Loading (g)			Number of Fertile Particles
		Uranium[b]	^{235}U	Thorium	
End plug 14-3	1250			<0.0233	<56
1	1250	0.0191	0.0014		
2	1250			0.0233	56
3	1250	0.0191	0.0014		
4	1250			0.0233	57
5	1250			0.0233	56
6	1250	0.0191	0.0014		
7	1250			0.0233	56
8	1250			0.0233	57
9	1250	0.0191	0.0014		
10	1250			0.0233	57
11	1250			0.0233	56
12	1250	0.0191	0.0014		
13	1250			0.0233	56
End plug 14-1	1250			<0.0233	<56
End Plug 15-3	1550			<0.0332	<80
14	1550	0.0268	0.0019		
15	1550			0.0332	80
16	1550	0.0268	0.0019		
17	1550			0.0332	81
18	1550			0.0332	81
19	1550	0.0268	0.0019		
20	1550			0.0332	83
21	1550			0.0332	82
22	1550	0.0268	0.0019		
23	1550			0.0332	81
24	1550			0.0332	81
25	1550	0.0268	0.0019		
26	1550			0.0332	85
End plug 15-1 RHMP[c]	1550			<0.0332	<80
End plug 26-1	1250	Inert			
27	1250			0.0228	42
28	1250	0.0129	0.0009	0.0145	
29	1250			0.0228	41
30	1250			0.0228	42
31	1250	0.0129	0.0009	0.0145	
32	1250			0.0228	43
33	1250			0.0228	42
34	1250	0.0129	0.0009	0.0145	
35	1250			0.0228	41
36	1250			0.0228	43

Table 2 (Continued)

Position[a]	Design Temperature (°C)	Loading (g)			Number of Fertile Particles
		Uranium[b]	^{235}U	Thorium	
37	1250	0.0129	0.0009	0.0145	
38	1250			0.0228	42
39-1	1250			0.0114	21
39-2	1250			0.0114	21
End plug 26-3	1250	Inerts			
End plug 28-1	900	Inerts			
40	900			0.0199	35
41	900	0.0056	0.0004	0.0104	
42	900			0.0199	35
43	900			0.0199	37
44	900	0.0056	0.0004	0.0104	
45	900			0.0199	37
46	900			0.0199	36
47	900	0.0056	0.0004	0.0104	
48	900			0.0199	36
49	900			0.0199	37
50	900	0.0057	0.0004	0.0104	
51	900			0.0199	37
52	900			0.0199	37
End plug 28-3	900				

[a] From top of capsule.

[b] All uranium is 7.07% enriched.

[c] Reactor horizontal midplane.

To meet objective 2, several batches of Triso-coated ThO_2 particles were also prepared in the 0.13-m coating furnace with the fritted gas distributor. Silicon carbide (SiC) deposition rates near 0.5 μm/min were achieved, and four batches were selected for irradiation in HT-34. The high deposition rates for the SiC layer were obtained by controlling the deposition temperature at 1550°C, increasing the hydrogen-to-methyltrichlorosilane ratio, and increasing the methyltrichlorosilane flux. Each particle batch selected for its SiC microstructure met the density requirements. The batches selected had a varied microstructure to permit study of the effects of microstructure on the irradiation

Table 3. Fabrication and Characterization Data for HT-34 Biso Particles

Batch	Hydrocarbon Gas	Diluent/ % Diluent	Deposition Temperature (°C)	LTI Thickness (μm)	Observed Gradient Density (Mg/m^3)	Correc ed Gradient Density (Mg/m^3)	Open Porosity (%)	Coating Rate (μm/min)	BAF_0	He/He Permeability	Defective Fraction		Crush Strength (kg)
											Cl_2 leach	Fission-gas Release	
A-762	Mixed[a]	He/67	1225	71.4	1.962	1.904	2.96	3.25	1.043	0.36[b]	1.3×10^{-5}	$<1 \times 10^{-6}$	2.7
A-765	Propylene	Ar/50	1350	78.6	1.915	1.858	2.99	3.14	1.035	3.34	1.8×10^{-5}	$<2 \times 10^{-6}$	3.2
A-780	Propylene	He/50	1350	78.2	1.864	1.773	4.92	4.03	1.022	0.37	4.2×10^{-6}	$<2 \times 10^{-6}$	2.9
A-782	Propylene	H_2/50	1350	88.4	1.855	1.810	2.43	2.95	1.026	0.27	5.2×10^{-5}	$<1 \times 10^{-6}$	3.3
A-785	Mixed	Ar/67	1225	76.3	1.872	1.815	3.02	3.05	1.035	0.32	8.6×10^{-7}	$<1 \times 10^{-6}$	2.5
A-786	Mixed	Ar/50	1225	88.0	1.897	1.826	3.75	3.67	1.030	0.36	8.9×10^{-7}	$<2 \times 10^{-6}$	3.2
A-787	Propylene	H_2/67	1350	80.5	1.738	1.691	2.71	2.68	1.031	0 35	1.5×10^{-5}	$<4 \times 10^{-6}$	2.9
A-806	Mixed	H_2/67	1225	70.6	1 943	1.878	3 33	2.82	1.036	0.38	1.1×10^{-6}	$<2 \times 10^{-6}$	2.2
OR-1975-T	Propylene	Ar/35	1310	83.0	1.982	ND[c]	ND	11.8	1.063[d]	0.19	ND	ND	ND
OR-2063-T	Propylene	CO_2/40–Ar/40	1325	84.5	2 002	ND	ND	11.5	1.028[d]	0.14	ND	ND	ND
OR-2730-1-H[b]	Propylene	Ar/40	1325	81.2	1.924	1.854	4.51	12.8	ND	0.26	NA[e]	NA	ND
OR-2722-1-H[b]	Propylene	Ar/67	1315	81.9	1.984	1 891	6.67	12.6	ND	0.27	NA	NA	ND
OR-2725-1-H[b]	Propylene	Ar/67	1315	82.2	1.998	1.910	4.42	11.7	ND	0.27	NA	NA	ND

[a] 54% acetylene, 46% propylene.

[b] Inert kernels.

[c] ND = not determined.

[d] Average for three particles.

[e] NA = not applicable.

performance of the coating (fission product retention and mechanical integrity). The characterization data for the SiC and the outer LTI (OLTI) coatings for the four batches selected are shown in Table 4.

Table 4. Characterization Data for ThO_2 Triso Particles for HT-34

Run	SiC				OLTI			
	Thickness (μm)	Deposition Rate (μm/min)	Density (Mg/m^3)	Fraction Defective (Hg intrusion)	Thickness (μm)	Observed Gradient Density (Mg/m^3)	Corrected Gradient Density (Mg/m^3)	Coating Rate (μm/min)
A-834	32.7	0.16	3.194	1.3×10^{-4}	43.5	1.898	1.752	5.30
A-835	36.5	0.45	3.193	1.4	47.7	1.883	1.767	5.81
A-836	34.3	0.28	3.158	1.5	46.6	1.853	1.736	5.68
A-837	35.5	0.39	3.183	1.4	49.0	1.890	1.771	5.98

The ThO_2 kernels had a nominal diameter of 500 μm, and the buffer layers ranged from 70 to 85 μm in thickness.

The Triso-coated ThO_2 particles were combined with the uranium (7%-enriched) driver particles (Table 5), and bonded-bed specimens were formed. These specimens were fabricated by the warm-molded process with a total particle loading of 35 vol %. The green rods were carbonized in

Table 5. Characteristics of Driver Particles[a] (OR-2576-H) in Rods for Capsule HT-34

Kernel (WAR[c] IRC-72)	
Stoichiometry	$U{\cdot}C_{0.40}{\cdot}O_{1.43}$
Nominal Conversion, %	30
Diameter, μm	376.1 (10.10)[b]
Density, Mg/m^3	3.26
Enrichment, %	7.073
Buffer	
Thickness, μm	53.7 (7.02)
Density, Mg/m^3	1.12
Inner LTI	
Thickness, μm	34.57 (3.20)
Density, Mg/m^3	1.939 (0.007)
SiC	
Thickness, μm	35.6 (1.50)
Density, Mg/m^3	3.200 (0.00066)
Coating Rate, μm/min	0.228
Outer LTI	
Thickness, μm	37.18 (2.60)
Density, Mg/m^3	2.020 (0.0046)
Coating Rate, μm/min	3.8

[a] WAR = weak-acid resin.

[b] Numbers in parentheses are standard deviations.

natural flake graphite at 1000°C and annealed at 1800°C. The annealed rods had a nominal diameter of 9.58 mm and a length of 7.0 mm.

Archive particles from batches OR-1975-T and OR-2013-T were also selected to resolve irradiation anomalies between these two similarly designed particle batches, which had been irradiated in capsules HT-18 and -19. Both particle batches were coated in a 25.4-mm conical coating tube at 1325°C. The hydrocarbon gas was propylene (C_3H_6) in each case. The difference between the two particle designs was that for OR-1975-T an argon diluent with a concentration of 67% was used, whereas OR-2013-T, used 50% CO_2 + 50% Ar as the diluent. The irradiation anomalies were that batch OR-1975-T, of reference design, failed extensively (~90%) in capsule HT-19, but OR-2013-T showed complete survival in both HT-18 and -19 (ref. 3).

IRRADIATION HISTORY

Irradiation capsule HT-34 was inserted into HFIR target position C-6 on July 25, 1977, to begin a scheduled five-cycle irradiation. The capsule was removed from this facility on November 23, 1977, after completing a total of 2685 h at full reactor power of 100 MW. The reactor power and irradiation history for the capsule are shown in Table 6. Total

Table 6. Reactor History During Operation of HT-34

HFIR Fuel Cycle	1977 Cycle Dates		Irradiation Time (h)	
	Begin	End	In Cycle	Total Accumulated
150	7/25	8/17	549	549
151	8/19	9/11	547	1096
152	9/11	10/4	545	1641
153	10/6	10/29	537	2178
154[a]	10/31	11/23	507	2685

[a]The reactor was shut down for 55.3 h (from 0500 11/7/77 to 1220 11/9/77) during cycle 154.

accumulated damage fluence and the calculated burnups for each test position are shown in Table 7.

Table 7. Calculated Burnup and Damage Fluence for HT-34

Specimen and Positions	Burnup [% Fissions per initial metal atom (FIMA)]			Fluence, >0.18 MeV (n/m^2)
	^{232}Th	^{235}U	^{238}U	
1, 52		85.0	10.8	4.8×10^{25}
2, 51	5.6			5.1
3, 50		85.2	11.7	5.5
4, 49	6.4			5.8
5, 48	6.7			6.1
6, 47		85.5	13.2	6.4
7, 46	7.3			6.7
8, 45	7.6			7.0
9, 44		85.7	14.6	7.2
10, 43	8.3			7.5
11, 42	8.6			7.7
12, 41		85.9	15.9	8.0
13, 40	9.2			8.2
14, 39		86.3	18.3	9.1
15, 38	10.7			9.2
16, 37		86.4	18.8	9.3
17, 36	11.0			9.4
18, 35	11.2			9.5
19, 34		86.5	19.5	9.6
20, 33	11.5			9.7
21, 32	11.6			9.8
22, 31		86.6	20.1	9.9
23, 30	11.9			10.0
24, 29	12.0			10.1
25, 28		86.7	20.5	10.2
26, 27	12.2			10.2

THERMAL ANALYSIS

Time-temperature relationships for the ORNL specimens irradiated in capsule HT-34 were calculated with the thermal modeling code HTCAP1 (modified version of HTCAP).[4] The ORNL specimens were in the form of loose particles in special holders and bonded fuel rods. Figures 3 and 4 are representative of the temperatures calculated for each specimen type irradiated in the high-temperature region. Peak irradiation temperatures were near 1500°C, and average-life temperatures were near 1350°C. The peak temperature for the rods occurred at beginning-of-life because of

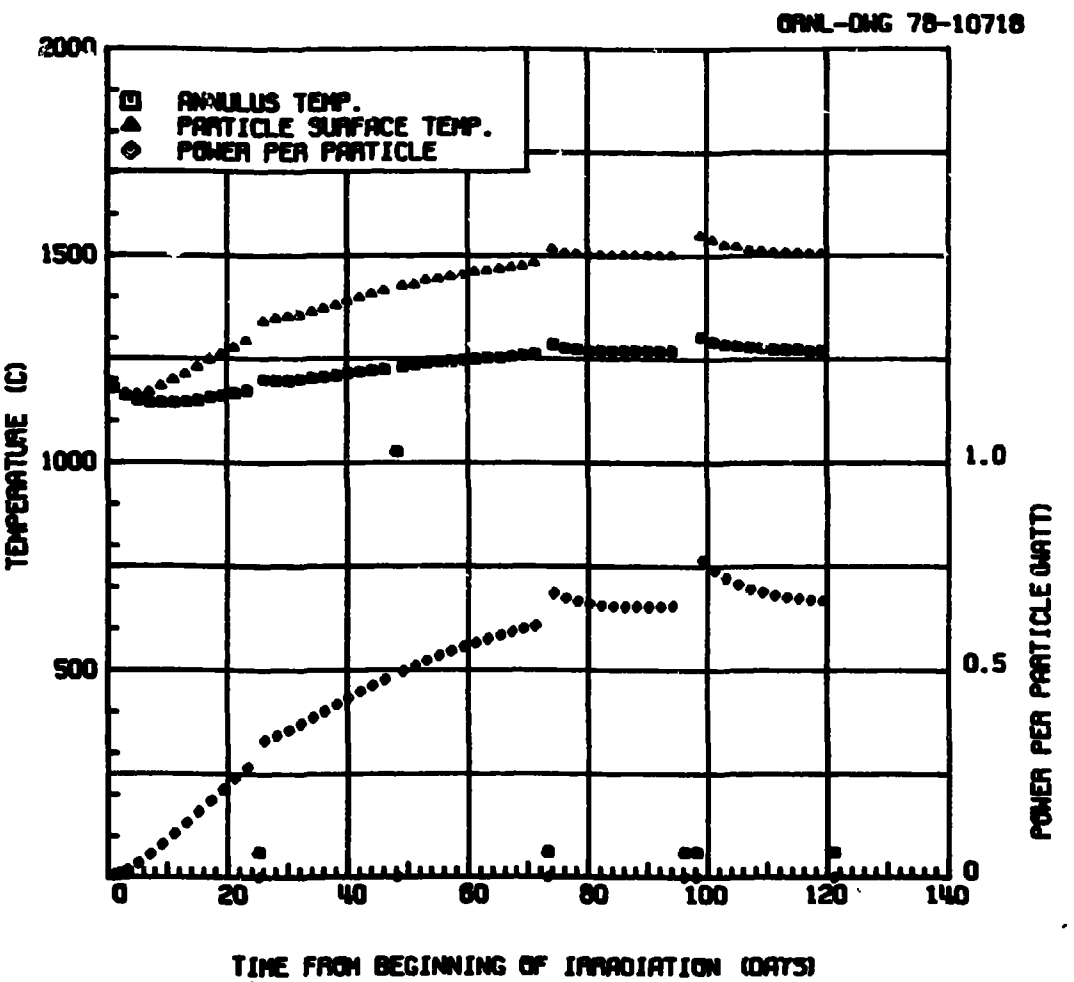

Fig. 3. HT-34 Particle Holder 30, Batch A-785, 816.5-μm Average Particle Diameter.

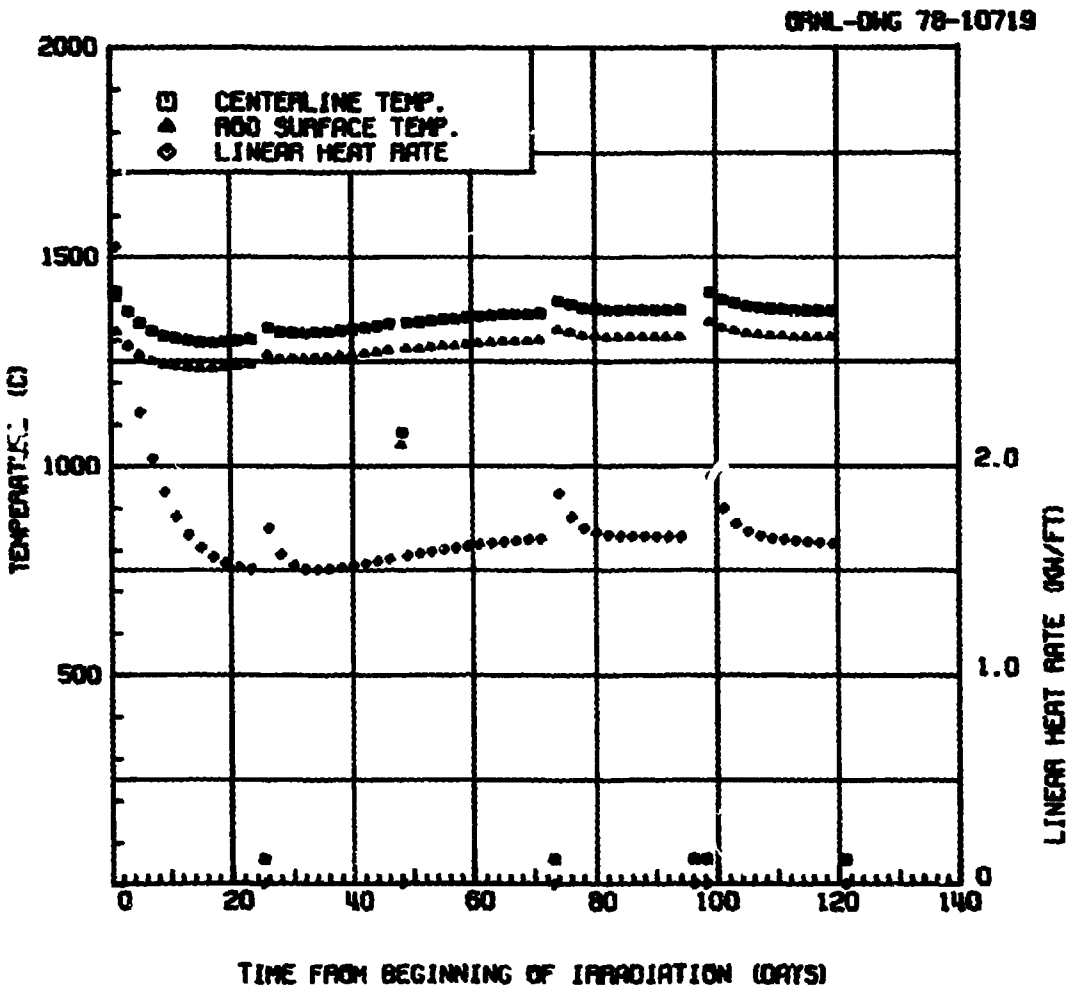

Fig. 4. HT-34 Fuel Rod 31, Batch A835 + OR-2576H, 743.1-μm Average Particle Diameter.

the fissile ^{235}U in the rod; for the loose particles, peak temperatures occurred at end-of-life. Figures 5 and 6 are representative of temperatures calculated for specimens irradiated in the low-temperature region of HT-34. Peak temperatures were near 1250°C for the loose particles and near 1100°C for the rods. Average-life temperatures were near 1175°C for the loose particles and 1050°C for the rods. Temperatures presented for the fuel rods represent peak and average centerline temperatures, not particle surface temperatures, as is the case for loose particles. (Thermal histories of all positions in HT-34 are given in Appendix A).

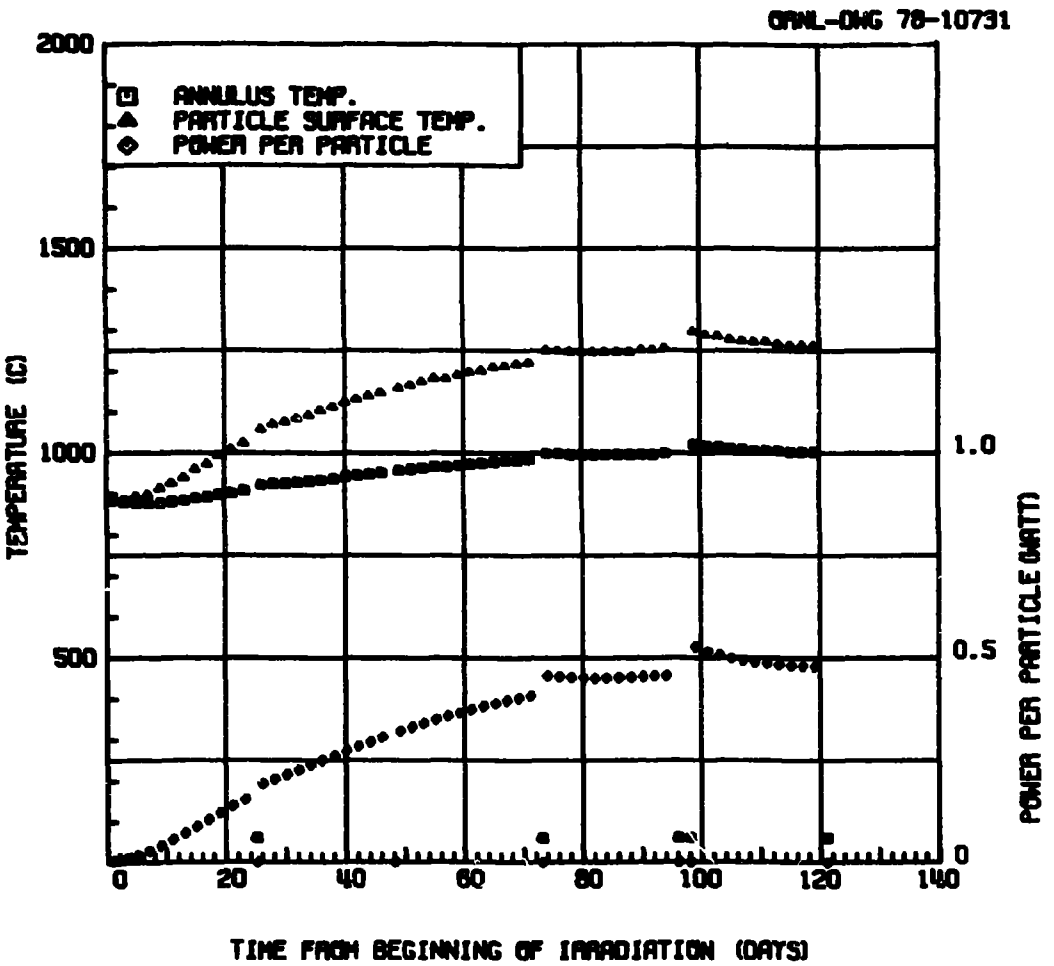

Fig. 5. HT-34 Particle Holder 43, Batch A-785, 816.5-μm Average Particle Diameter.

The temperatures just quoted are 100 to 200°C higher than the 1250 and 900°C design temperatures of the two temperature regions. Calculations were also made on the ORNL section with the fissile and fertile metal removed. In these cases, the only source of heat generation was from gamma heating [peak value of about 35 W/g at HMP (horizontal midplane of the reactor)]. For the high-temperature region, the peak temperature was about 1025°C; for the low-temperature region, it was about 825°C (these values are for the particle holders; fuel rod temperatures were about 25°C higher). These temperatures appear to be the minimum temperatures for target capsules without fissile or fertile fuel.

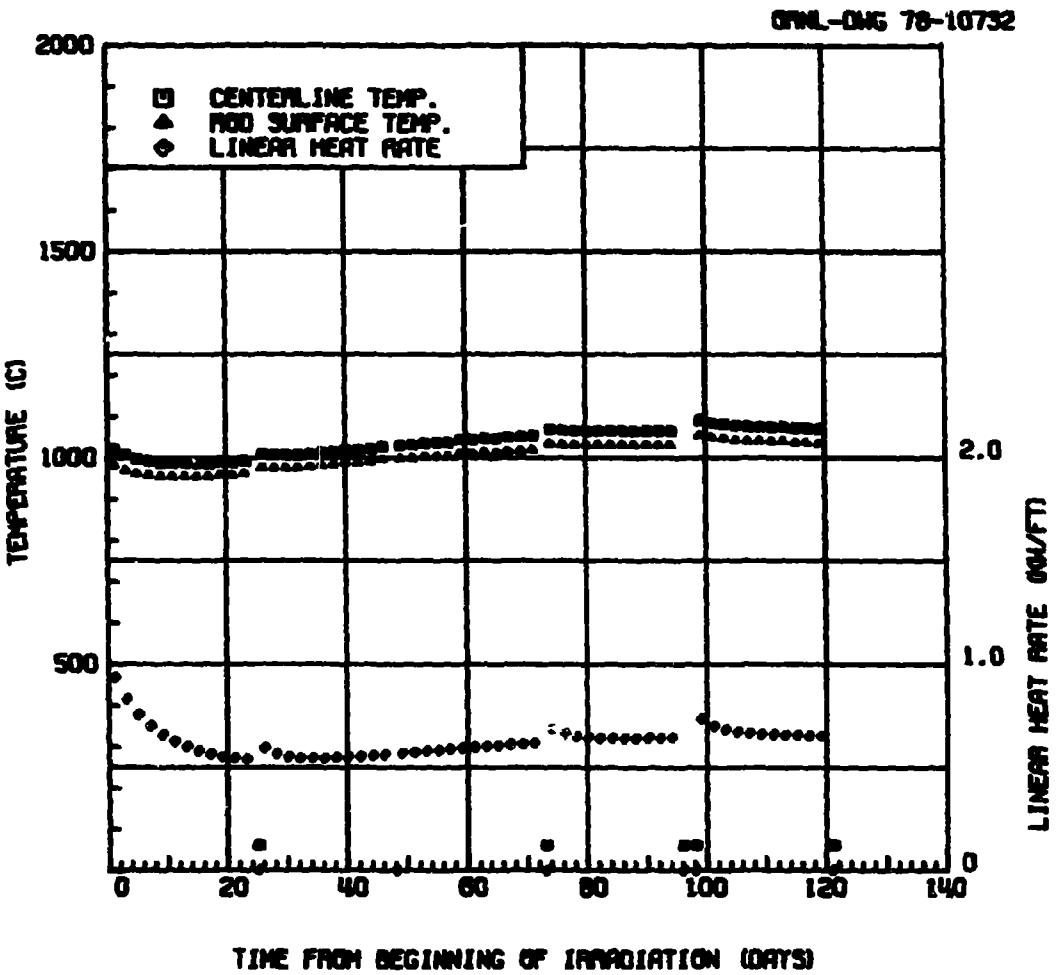

Fig. 6. HT-34 Fuel Rod 44, Batch A835 + OR-2576H, 743.1-μm Average Particle Diameter.

For the high-temperature region, a third case was run in which only the uranium driver fuel was considered. The peak holder temperatures increased to about 1270°C at the HMP and decreased to about 1130°C at about 13 cm from the HMP. These temperatures occurred at beginning-of-life only; temperatures at end-of-life had reduced to 1140°C at the HMP and 1075°C at 13 cm from the HMP. Similar temperature changes would also occur in the low-temperature region of the capsule. In each of these cases, end-of-life was after five full HFIR cycles.

POSTIRRADIATION EXAMINATION

Capsule HT-34 was received at the High-Radiation-Level Examination Laboratory (HRLEL) in mid-December 1977 for postirradiation examination (PIE). Before disassembly, gross-gamma scans of the capsule were recorded, and a sample of the internal gas was analyzed. The gamma scans showed no unusual effects; the results from the gas sample showed that the cladding remained gastight throughout the irradiation test.

After containment removal, the four graphite magazines were visually and dimensionally inspected. A representative from GA was present to oversee the disassembly, retrieval, and visual examination of the upper magazines from the capsule. The exterior of the magazines appeared to be in good condition, but there was an excessive amount of soot in the capsule. Results from the dimensional inspections are given in Appendix B.

The two low-temperature magazines were unloaded without difficulty. However, the end plugs in the high-temperature magazines were stuck, and during their removal, the ends of the magazines were broken. Particle holders and fuel rods could not be removed until the magazines were slit and split open. No particles were lost from the end plugs because the graph-foil plugs remained in place.

The appearance of the bonded fuel rods from both the low- and high-temperature regions was good: no debonding was noted. Five of the loose-particle holders in the high-temperature regions were broken during removal; however, most of the particles in these holders were recovered. There was some difficulty in retrieving the loose particles from the low-temperature holders. Scanning electron microscopy examination indicated that the cause of the problem was a buildup of an unidentified granular material in the annulus, where particles are held (Fig. 7). Attempts to identify this material through electron microprobe analysis were unsuccessful.

The loose coated particles from the ORNL portion of the experiment were visually examined; the results are given in Table 8. As shown, numerous pressure-vessel failures were observed; most of them occurred in the low-temperature region. It is believed that the failures are a result of the particles not being annealed before irradiation. (In the

Fig. 7. Scanning Electron Micrograph of Loose-Particle Holder 51 from Capsule HT-34, 15x.

Table 8. Summary of Results from Visual Examination of ORNL Biso-coated Fertile Particles in HT-34

Capsule Position	Batch	Number of Coated Particles				Failure Mode[b]	Failed[a] (%)
		Loaded	Recovered		Unaccounted For		
			Intact	Failed[a]			
High-temperature Magazine							
27	A-765	42	31	6	5	PV	14-26
29	A-780	41	39	1	1	PV	2-5
30	A-785	42	37	1	4	PV	2-12
32	A-806	43	41	2	0	PV	5
33	A-762	42	34	4	4	PV	10-19
35	A-782	41	41	0	0	None	0
36	A-786	43	43	0	0	None	0
38	A-787	42	42	0	0	None	0
39-1	OR-1975-T	21	16	3	2	FND	14-24
39-2	OR-2013-T	21	21	0	0	None	0
Low-temperature Magazine							
40	A-765	35	25	10	0	PV	29
42	A-780	35	28	7	0	PV	20
43	A-785	37	29	6	2	PV	16-(22)[d]
45	A-806	37	34	3	0	PV	8
46	A-762	36	23	10	3	PV	28-36
48	A-782	36	31	5	0	PV	14
49	A-786	37	35	1	1	PV	3-5
51	A-787	37	22	0	15		0-(27)[d]
52	OR-1975-T	37	19	1	17	PV	3-(32)[d]

[a] Estimated from coating fragments.

[b] PV = pressure vessel; FND = fast-neutron damage.

[c] First numbers are based on coating fragments; second numbers are based on fragments + unaccounted-for particles.

[d] Thirty-three intact particles found in common container used to store holders from low-temperature magazines.

past all loose particles were annealed at 1800°C for at least 10 min.) Evidently, annealing is necessary to relieve stresses in the pyrocarbon coatings that are introduced during the coating process; this would also explain why the particles in high-temperature regions had higher survival rates (i.e., the pyrocarbon coating stresses were partially relieved in the reactor). The surviving particles appeared to be in good condition.

The issue of whether or not particles need to be annealed after coating has been actively discussed. Experience at ORNL has shown that particles coated by using a conical gas distributor in the coating furnace frequently experience many breakages or cracks during postfabrication characterization (chlorine leach, etc.), unless the particles are annealed at 1800°C before cooling the coating furnace.[2] It was, therefore, ORNL's position that annealing was a necessary step, so it was routinely done on all batches fabricated, as indicated earlier. Studies at ORNL have shown that annealing the coated particles that were deposited using a conical distributor increases the crushing strength. However, ORNL has since switched to a fritted gas distributor. The HT-34 particles were coated using the frit. Studies on coated particles prepared by using frit distributors showed essentially no difference in particle breakage or crushing strength for annealed vs unannealed particles.[2] Because the particles are effectively annealed during fuel rod fabrication, it was decided that annealing after particle coating was no longer necessary. The HT-34 experience has caused us to question the validity of this assumption. We have speculated that the cause of the pressure-vessel failures in the HT-34 specimens is the lack of annealing. Another experiment would be required to make a definitive statement about the need for annealing loose particles before irradiation. That experiment would be for irradiating annealed and unannealed particles from the same batch under identical irradiation conditions. Because of funding limitations, it is unlikely that such an experiment will be conducted.

The samples of particles from the two OR batches that were annealed after coating were tested in an earlier HT series[3] and showed results similar to those from HT-34. Coatings for Batch OR-2013-T were deposited by using propylene and 50% CO_2 + 50% Ar as a diluent. Batch OR-1975-T was coated using propylene + 100% Ar diluent. The deposition rates, temperatures, gas concentrations, and gas fluxes were equivalent.

The range in failure rate shown for particles irradiated in low-temperature magazine positions 51 and 52 is believed to be too high; 38 particles were unaccounted for in this magazine, but 33 intact particles were found in the storage container used for the "empty" particle holders.

GAMMA ANALYSIS OF BISO- AND TRISO-COATED ThO_2 PARTICLES

The ThO_2 particles from nearly every position were examined by the Irradiated-Microsphere Gamma Analyzer (IMGA) system.[5] These included particles from GA (positions 2, 4, 5, 7, 8, 10, 11, 13, 15, 17, 20, and 26) and ORNL (positions 27-52). Measurements of the gamma-ray spectrum from irradiated fuel particles have been useful in determining the performance and the fission product retention characteristics of the particles.[6,7] Measurement is accomplished by taking the ratio of volatile to stable fission products (e.g., $^{137}CS/^{95}Zr$). The ratios can then be compared with calculated theoretical ratios, and an assessment of the particle batch can be made. The calculated ratios were determined by using a modified version[8] of an existing computer code.[9] Results on the calculated ratios for $^{137}Cs/^{95}Zr$, $^{134}Cs/^{137}Cs$, and $^{144}Ce/^{95}Zr$ for the ORNL positions are shown in Table 9.

The ThO_2 particles that were irradiated and examined for GA were all Triso coated. Results of the gamma analysis of these particles have been forwarded to GA, and they will interpret the results in relation to the particles' fabrication.

Biso-coated ThO_2 Particles

After the ORNL Biso-coated ThO_2 particles were visually examined, those judged intact were separated and gamma analyzed. The results on the $^{137}Cs/^{95}Zr$, $^{134}Cs/^{137}Cs$, and $^{144}Ce/^{95}Zr$ activity ratios are presented in Tables 10, 11, and 12.

As shown in Table 10, the Biso-coated ThO_2 particles exhibited very poor ^{137}Cs retention in the high-temperature, high-burnup region of the capsule (positions 27-39) and very good retention in the low-temperature, low-burnup region (positions 40-52). In fact, on a failure-fraction

Table 9. Calculated Fission Product Activity Ratios[a] for ORNL ThO_2 Positions in HT-34

Position[b]	$^{137}Cs/^{95}Zr$	$^{134}Cs/^{137}Cs$	$^{144}Ce/^{95}Zr$
27	9.477×10^{-3}	1.582	2.566×10^{-1}
28	9.476	1.561	2.565
29	9.476	1.539	2.563
30	9.476	1.538	2.561
31	9.477	1.520	2.558
32	9.477	1.501	2.555
33	9.477	1.500	2.554
34	9.477	1.482	2.552
35	9.477	1.464	2.549
36	9.477	1.436	2.547
37	9.478	1.431	2.545
38	9.479	1.426	2.542
39	9.483	1.420	2.530
40	9.488	1.417	2.517
41	9.491	1.405	2.513
42	9.494	1.392	2.510
43	9.496	1.360	2.503
44	9.502	1.329	2.597
45	9.507	1.297	2.492
46	9.515	1.290	2.487
47	9.521	1.257	2.479
48	9.528	1.224	2.471
49	9.529	1.169	2.465
50	9.532	1.150	2.460
51	9.535	1.131	2.455
52	9.540	1.067	2.445

[a] Ratio of disintegrations per second corrected to time out of reactor.

[b] High-temperature, high-burnup positions 27-39; low-temperature, low-burnup positions 40-52.

basis, the high-temperature, high-burnup particles had 100% failure (loss of a significant portion of the fission product inventory), and the low-temperature, low-burnup particles had 0% failure. However, the analysis of the particles cannot be as simple as the failure fraction makes it appear because even bare ThO_2 kernels do not release all their ^{137}Cs during irradiation.[10]

These results were coupled with results from capsules HT-12 through HT-15 and are summarized in Fig. 8. As shown, the retention of ^{137}Cs

Table 10. Measured $^{137}Cs/^{95}Zr$ Activity Ratio for ORNL Biso-coated ThO_2 Particles

Position[a]	Measured $^{137}Cs/^{95}Zr$ Ratio				
	Minimum	Maximum	Mean	Standard Deviation (%)	Mean Fraction of Calculated Ratio[b] (%)
27	9.264×10^{-4}	6.520×10^{-3}	3.336×10^{-3}	43.70	35.2
29	8.395×10^{-4}	4.609×10^{-3}	2.635×10^{-3}	35.28	27.8
30	1.762×10^{-3}	6.270×10^{-3}	4.269×10^{-3}	31.72	45.1
32	8.827×10^{-4}	5.079×10^{-3}	2.652×10^{-3}	35.36	28.0
33	6.863×10^{-4}	5.979×10^{-3}	2.605×10^{-3}	47.47	27.5
35	1.185×10^{-3}	4.342×10^{-3}	2.574×10^{-3}	29.72	27.2
36	1.102×10^{-3}	4.823×10^{-3}	2.858×10^{-3}	34.15	30.2
38	9.183×10^{-4}	2.485×10^{-3}	1.458×10^{-3}	21.84	15.4
39-1	1.489×10^{-3}	5.794×10^{-3}	4.020×10^{-3}	25.95	42.4
39-2	1.518×10^{-3}	6.149×10^{-3}	3.458×10^{-3}	47.94	36.5
40	9.184×10^{-3}	9.990×10^{-3}	9.760×10^{-3}	2.17	102.9
42	9.447×10^{-3}	1.000×10^{-2}	9.811×10^{-3}	1.09	103.3
43	9.497×10^{-3}	9.925×10^{-3}	9.759×10^{-3}	0.97	102.8
45	9.688×10^{-3}	9.928×10^{-3}	9.815×10^{-3}	0.62	103.3
46	9.560×10^{-3}	1.041×10^{-2}	1.016×10^{-2}	1.68	106.8
48	9.562×10^{-3}	9.789×10^{-3}	9.685×10^{-3}	0.55	101.7
49	9.722×10^{-3}	9.947×10^{-3}	9.831×10^{-3}	0.56	103.2
51	9.555×10^{-3}	9.819×10^{-3}	9.707×10^{-3}	0.70	101.8
52	9.741×10^{-3}	1.004×10^{-2}	9.873×10^{-3}	0.81	103.5

[a] High-temperature, high-burnup positions 27-39; low-temperature, low-burnup positions 40-52.

[b] The range of fractional inventories can be determined by comparing the calculated ratio with the minimum and maximum measured values.

varies with temperature and burnup. Thus, at low burnups [<3% fissions per initial metal atom (FIMA)], ^{137}Cs release apparently does not become serious until temperatures well above 1400°C are reached. (It should be noted that the irradiation temperatures used are time averaged and do not represent temperature excursions. Therefore, one would not expect an immediate release to the level shown in Fig. 8 if the particle were operated at, for example, 1500°C for a short time.) At high burnups (>10% FIMA), high ^{137}Cs releases were observed at temperatures as low as 1250°C. The spread in the arbitrary burnup ranges shown in Fig. 8 are due to differences between samples in fast neutron fluence, pyrocarbon coating properties and dimensions, and individual temperature transients during irradiation.

The trend displayed in the $^{137}Cs/^{95}Zr$ results is also evident in the $^{134}Cs/^{137}Cs$ results shown in Table 11. That is, the particles in the

Table 11. Measured $^{134}Cs/^{137}Cs$ Activity Ratio for ORNL Biso-coated ThO_2 Particles

Position[a]	Measured $^{134}Cs/^{137}Cs$ Ratio				
	Minimum	Maximum	Mean	Standard Deviation (%)	Mean Fraction of Calculated Ratio[b] (%)
27	4.082×10^{-1}	1.342	9.682×10^{-1}	29.32	61.2
29	4.154	1.269	9.220	23.80	59.9
30	5.962	1.392	1.124	17.67	73.1
32	4.213	1.295	9.808×10^{-1}	19.98	65.3
33	3.776	1.403	9.875	25.35	65.8
35	3.771	1.212	8.445	20.81	57.7
36	3.352	1.173	8.318	24.40	57.9
38	2.729	8.251×10^{-1}	5.387	24.58	37.8
39-1	5.401	1.226	9.757	18.53	68.7
39-2	4.444	1.305	8.778	33.32	61.8
40	1.384	1.435	1.409	0.93	99.4
42	1.376	1.414	1.392	0.79	101.6
43	1.343	1.384	1.366	0.73	100.1
45	1.267	1.314	1.293	0.94	99.8
46	1.267	1.304	1.290	0.73	100.7
48	1.211	1.236	1.223	0.56	99.9
49	1.153	1.182	1.169	0.62	100.0
51	1.120	1.155	1.135	0.76	100.4
52	1.048	1.085	1.067	0.87	100.0

[a] High-temperature, high-burnup positions 27-39; low-temperature, low-burnup positions 40-52.

[b] The range of fractional inventories can be determined by comparing the calculated ratio with the minimum and maximum measured values.

high-temperature, high-burnup region of the capsule showed substantial fission product release (as indicated by the $^{134}Cs/^{137}Cs$ activity ratio), whereas no substantial release from the particles was evident in the low-temperature, low-burnup region.

The $^{134}Cs/^{137}Cs$ activity ratio is an indicator of ^{133}Xe fission-gas behavior.[5] Cesium-134 is an activation product of ^{133}Cs, and both have very low direct fission product yields. Therefore, essentially all the ^{134}Cs observed has 5.29-d ^{133}Xe as a precursor. Assuming that ^{134}Cs and ^{137}Cs migrate at similar rates, any deviation in the $^{134}Cs/^{137}Cs$ ratio from the expected value is due to an increase in release of ^{133}Xe.

The results in Table 11 show that the particles in the high-temperature, high-burnup region were releasing ^{133}Xe during irradiation. This indicates that, at those levels, the pyrocarbon coatings on the particles were permeable to fission gases. The particles in the low-temperature, low-

Table 12. Measured $^{144}Ce/^{95}Zr$ Activity Ratio for ORNL Biso-coated ThO_2 Particles

Position[a]	Measured $^{144}Ce/^{95}Zr$ Ratio				
	Minimum	Maximum	Mean	Standard Deviation (%)	Mean Fraction of Calculated Ratio[b] (%)
27	8.006×10^{-2}	2.519×10^{-1}	2.169×10^{-1}	13.41	84.5
29	2.118×10^{-1}	2.441	2.234	2.16	87.2
30	1.024	2.407	2.128	9.17	83.1
32	2.147	2.359	2.246	1.80	87.9
33	1.393	2.749	2.235	9.37	87.5
35	2.043	2.150	2.110	1.14	82.8
36	2.132	2.233	2.181	0.99	85.6
38	2.100	2.194	2.162	0.86	85.1
39-1	2.031	2.080	2.062	0.66	81.5
39-2	2.058	2.137	2.103	0.94	83.1
40	2.042	2.128	2.096	1.10	83.3
42	2.085	2.236	2.192	1.37	87.3
43	2.111	2.188	2.146	0.78	85.7
45	2.109	2.181	2.143	0.83	86.0
46	2.083	2.302	2.190	1.71	88.1
48	2.079	2.169	2.127	0.83	86.2
49	2.088	2.181	2.142	0.89	86.9
51	1.986	2.095	2.064	1.49	84.1
52	2.175	2.218	2.196	0.53	89.8

[a] High-temperature, high-burnup positions 27-39; low-temperature, low-burnup positions 40-52.

[b] The range of fractional inventories can be determined by comparing the calculated ratio with the minimum and maximum measured values.

burnup region, on the other hand, were not releasing ^{133}Xe during irradiation. However, it cannot be said that those coatings were impermeable to all fission gases. The release of ^{133}Xe from the ThO_2 kernels at the lower temperatures and burnups may have been slow enough for nearly all the ^{133}Xe to decay before it could be released; thus, no deviation in the $^{134}Cs/^{137}Cs$ activity ratio is evident.[10] Because ^{133}Xe is one of the longest-lived fission gases produced during irradiation, one can conclude that other less stable radioactive fission gases (e.g., ^{85m}Kr, ^{87}Kr, ^{88}Kr, ^{135}Xe) will also decay before they can be released from the particles. As long as ThO_2 particles are maintained at moderate temperatures and burnups, no release of radioactive fission gases is expected from permeable pyrocarbon coatings. Note, however, that the stable fission gases may become activated into radioactive species (e.g., ^{84}Kr into ^{85m}Kr) after

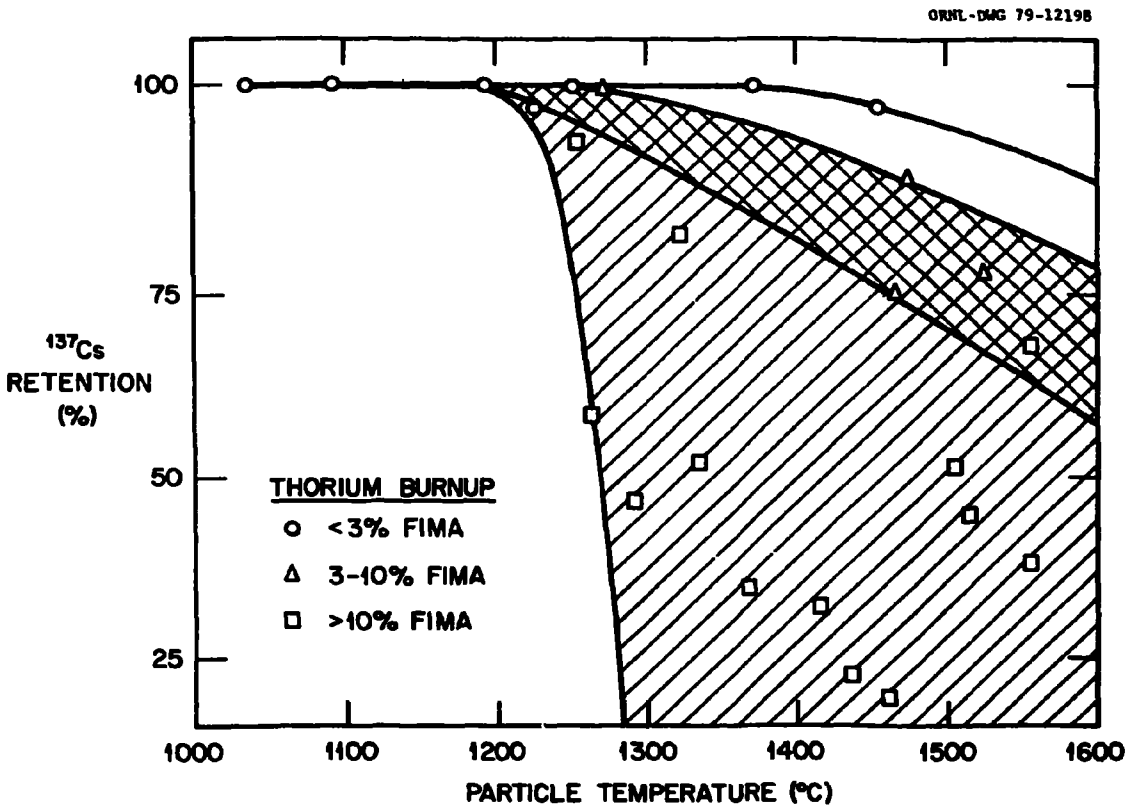

Fig. 8. Correlation Between ^{137}Cs Retention in Biso-coated ThO_2 Particles, Temperature, and Burnup.

release by permeable pyrocarbon coatings; thus, permeability should still be considered a potential problem.

The results on the ^{144}Ce/^{95}Zr activity ratio were surprising: there were ^{144}Ce losses of up to 18.5% from the particles. However, it is believed that the discrepancy could be attributed to errors in the fission yield of ^{144}Ce or to the neutron capture cross section in the HFIR target region being greater than expected.

We first thought that part of the problem was miscalculation of the attenuation of the ^{144}Ce peak at 133.5 keV, so we calculated some activity ratios at a ^{144}Ce peak of 696.5 keV. In every case, the two independently calculated ratios coincided within 1 to 2%. Definitely, attenuation through the coatings was not the problem.

The conclusion that the calculated ratios were in error is drawn because all the apparent losses are nearly identical, whereas if they

were real, we would expect some change with increasing temperature or other irradiation conditions. Additionally, the standard deviations were nearly all very low, which is generally indicative of no release. In other cases in which fission product loss definitely occurred, as indicated by the $^{137}Cs/^{95}Zr$ ratios, the standard deviations increased with increasing release. Thus, we believe that no ^{144}Ce was released from ThO_2 particles during irradiation.

Triso-coated ThO_2 Particles

The ORNL Triso-coated ThO_2 particles were contained in the driver rods in the ORNL half of the capsule. These rods were electrolytically deconsolidated to retrieve the particles after irradiation. Results on the $^{137}Cs/^{95}Zr$, $^{134}Cs/^{137}Cs$, and $^{144}Ce/^{95}Zr$ activity ratios are shown in Tables 13, 14, and 15.

As shown in Table 13, a failure-fraction determination based on the $^{137}Cs/^{95}Zr$ activity ratio was made, which showed failures occurring in three of the four high-temperature, high-burnup positions. The SiC coating on these particles varied in deposition rates. A rough correlation between deposition rate and failure fraction (Fig. 9) shows that the best performer at the higher temperatures and burnups, was the SiC with the highest deposition rate (0.45 μm/min). At the lower temperatures and burnups, all the SiCs performed equally well.

The results on the $^{134}Cs/^{137}Cs$ activity ratio (Table 14) appeared similar to those on the $^{137}Cs/^{95}Zr$ ratio; the only deviations from the theoretical values occurred in the high-temperature, high-burnup region. Failure fractions were again calculated based on the $^{134}Cs/^{137}Cs$ ratio. The only difference between these and the failure fractions based on the $^{137}Cs/^{95}Zr$ ratio occurs at position 28, where only 8 failures were observed vs 11 failures for the $^{137}Cs/^{95}Zr$ ratio. This finding indicates that the SiC coating on 8 of the particles failed early enough (and ^{133}Xe was released fast enough) to cause deviations in the $^{134}Cs/^{137}Cs$ ratio. In the other 3 particles at position 28, the SiC coating failed late enough during irradiation that most of the ^{133}Xe decayed to ^{133}Cs; no

Table 13. Measured $^{137}Cs/^{95}Zr$ Activity Ratio for ORNL Triso-coated ThO_2 Particles

Position	Measured $^{137}Cs/^{95}Zr$ Ratio						
	Minimum	Maximum	Mean	Standard Deviation (%)	Calculated Ratio	Mean Fraction of Calculated[a] Ratio (%)	Failure Fraction[b] (%)
28	2.782×10^{-3}	9.857×10^{-3}	7.985×10^{-3}	33.47	9.476×10^{-3}	84.3	35.5 (11/31)
31	9.548	9.819	9.682	0.58	9.477	102.2	0 (0/33)
34	2.775	9.851	9.228	19.07	9.477	97.4	8.6 (3/35)
37	2.695	1.006×10^{-2}	9.586	15.06	9.478	101.1	4.0 (1/25)
41	9.427	9.737×10^{-3}	9.579	0.87	9.491	100.9	0 (0/24)
44	9.633	9.830	9.709	0.59	9.502	102.2	0 (0/14)
47	9.539	9.794	9.622	0.61	9.521	101.1	0 (0/22)
50	9.723	9.895	9.809	0.54	9.532	102.9	0 (0/22)

[a] The range of fractional inventories can be determined by comparing the calculated ratio with the minimum and maximum measured values.

[b] Numbers in parentheses are number of failed particles per number of particles examined. Failures are defined as those particles >3 standard deviations below the mean.

Table 14. Measured $^{134}Cs/^{137}Cs$ Activity Ratio for ORNL Triso-coated ThO_2 Particles

Position	Measured $^{134}Cs/^{137}Cs$ Ratio						
	Minimum	Maximum	Mean	Standard Deviation (%)	Calculated Ratio	Mean Fraction of Calculated[a] Ratio (%)	Failure Fraction[b] (%)
28	9.893×10^{-1}	1.653	1.492	14.43	1.561	95.6	25.8 (8/31)
31	1.589	1.623	1.605	0.61	1.520	105.6	0 (0/33)
34	1.074	1.590	1.533	7.27	1.483	103.4	8.6 (3/35)
37	1.100	1.570	1.529	5.92	1.432	106.8	4.0 (1/25)
41	1.420	1.594	1.473	3.20	1.406	104.8	0 (0/24)
44	1.349	1.388	1.366	0.78	1.329	102.8	0 (0/14)
47	1.266	1.311	1.283	0.97	1.257	102.1	0 (0/22)
50	1.108	1.155	1.130	0.94	1.150	98.3	0 (0/22)

[a] The range of fractional inventories can be determined by comparing the calculated ratio with the minimum and maximum measured values.

[b] Numbers in parentheses are number of failed particles per number of particles examined. Failures are defined as those particles >3 standard deviations below the mean.

Table 15. Measured $^{144}Ce/^{95}Zr$ Activity Ratio for ORNL Triso-coated ThO_2 Particles

Position	Measured $^{144}Ce/^{95}Zr$ Ratio				
	Minimum	Maximum	Mean	Standard Deviation (%)	Mean Fraction of Calculated Ratio[a] (%)
28	1.873×10^{-1}	2.441×10^{-1}	2.126×10^{-1}	5.96	82.9
31	1.708	2.214	2.020	7.79	79.0
34	1.873	2.309	2.219	4.53	87.0
37	1.825	2.300	2.134	7.31	83.9
41	1.766	2.149	2.055	5.84	81.8
44	1.936	2.214	2.117	4.36	81.5
47	2.025	2.170	2.114	1.60	85.3
50	1.792	2.315	2.151	4.46	87.4

[a]The range of fractional inventories can be determined by comparing the calculated ratio with the minimum and maximum measured values.

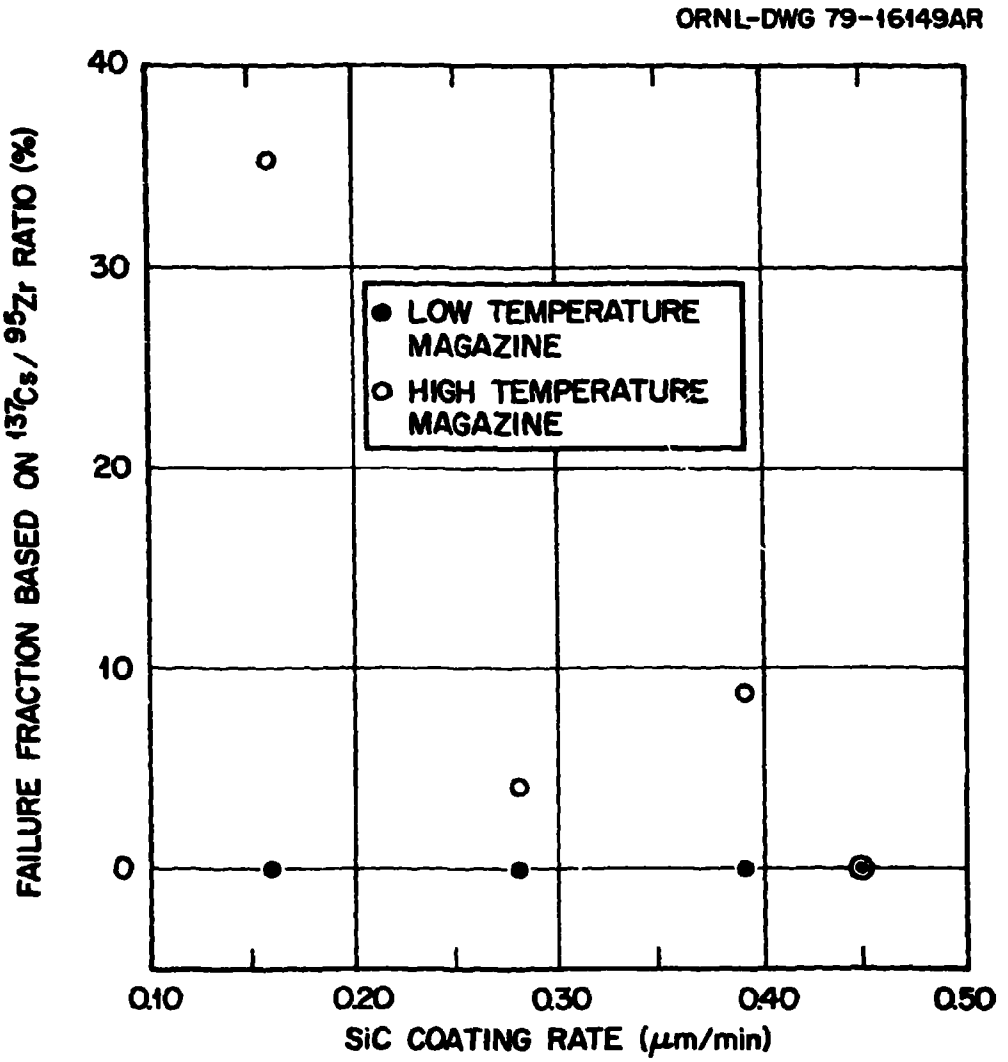

Fig. 9. Failure of SiC Layers in Triso-coated ThO_2 Particles as a Function of SiC Coating Rate.

perceptible deviation in the $^{134}Cs/^{137}Cs$ ratio occurred. In the other two positions where SiC failure was observed, the failures were early enough and the ^{133}Xe release fast enough for the failures to be reflected in the $^{134}Cs/^{137}Cs$ ratio.

The $^{144}Ce/^{95}Zr$ ratio results shown in Table 12 are similar to those of the Biso-coated ThO_2 particles. For the same reasons, we concluded that no ^{144}Ce loss occurred.

FISSION-GAS-CONTENT MEASUREMENTS

Six Biso-coated ThO_2 particles were selected from each ORNL holder for fission-gas-content measurements with the aid of the Postirradiation Gas Analyzer (PGA) system.[11] Each particle was visually inspected for defects and processed through the IMGA system. The identity of each particle was maintained to compare the quantity of fission-gas species measured by the PGA system with the total amount generated during irradiation. The particles were broken individually at room temperature, and the quantity of fission gas released at breakage was measured. The quantity of gas measured was essentially all that had been released by the kernel to the void space within the particle but retained by the OLTI layer, that is, a test for permeable or gastight OLTI layers. During the measurements, it was proven that the amount of additional fission gas released at kernel breakage was insignificant in determining whether particles were gastight or permeable. The results of the PGA measurements are presented in Table 16. By examining the quantities of gases in the Σ Kr and Σ Xe columns, it is evident that many of the particles were very permeable, either as the total particle sample (see position 52) or as individual particles within a particle sample (see position 27). A summary of the condition of the Biso coatings is given in Table 17. Note that particles from only one batch (A-780) remained gastight in both the high- and low-temperature magazines. Also, it is apparent from Table 17 that particles from four of the eight A batches in the high-temperature magazine remained gastight, whereas only one in the low-temperature magazine remained gastight. What appeared to be a similar anomaly was observed during the visual inspection of the particles after capsule disassembly — significantly more failures were noted in the low-temperature magazine. At that time it was speculated that residual stresses from the coating process had been partially annealed out in the high-temperature magazine while in HFIR. These particles received no postcoating anneal before irradiation. Particles from six of the eight A batches were annealed, included in HRB-14, and are currently being evaluated with the PGA system.

Table 16. Results of Fission-gas Inventory Measurements on Particles from Experiment HT-34

Position-Particle	Batch	Quantity of Gas (n moles)									
		^{83}Kr	^{84}Kr	^{86}Kr	Σ Kr	^{131}Xe	^{132}Xe	^{134}Xe	^{136}Xe	Σ Xe	Xe/Kr
						High-temperature Magazine					
27-1	A-765	0.46	3.36	4.20	8.02	2.62	9.83	10.10	19.44	42.00	5.23
27-2		0.52	3.96	4.84	9.33	3.06	11.45	11.88	22.86	49.25	5.28
27-3		0.49	3.65	4.58	8.72	2.78	10.22	10.60	20.45	44.04	5.05
27-4		0.63	4.64	5.84	11.12	3.51	13.23	13.60	26.15	56.49	5.08
27-5		0.01	0.01	0.02	0.04	0.01	0.3	0.01	0.04	0.09	2.25
27-6		0.49	3.80	4.50	8.80	2.75	10.15	10.78	20.78	44.46	5.05
29-1	A-780	0.46	3.20	3.95	7.61	2.59	9.24	9.65	18.57	40.05	5.26
29-2		0.49	3.73	4.50	8.72	2.82	10.19	10.57	20.61	44.20	5.07
29-3		0.54	3.75	4.61	8.90	3.01	10.75	11.31	22.09	47.17	5.30
29-4		0.63	4.49	5.51	10.63	3.62	13.07	13.55	25.76	56.01	5.27
29-5		0.69	4.74	5.70	11.14	3.77	13.85	14.60	27.85	60.06	5.39
29-6		0.66	4.56	5.60	10.82	3.62	13.20	14.37	27.23	58.42	5.40
30-1	A-785	0.40	2.92	3.45	6.77	2.16	7.97	8.05	15.67	33.85	5.00
30-2		0.54	3.61	4.42	8.56	2.79	10.11	10.40	20.23	43.54	5.08
30-3		0.48	3.73	4.59	8.81	2.89	10.76	10.95	21.69	46.30	5.25
30-4		0.52	3.93	4.81	9.27	2.92	10.96	11.16	21.66	46.70	5.04
30-5		0.50	3.74	4.62	8.86	2.99	10.90	11.12	21.67	46.68	5.27
30-6		0.57	4.15	5.06	9.76	3.09	11.47	11.57	22.65	48.77	4.98
32-1	A-806	0.08	0.33	0.50	0.92	0.36	1.01	0.95	2.08	4.40	4.79
32-2		0.16	0.84	1.17	2.17	1.03	2.46	2.50	4.94	10.93	5.04
32-3		0.21	0.90	1.20	2.31	0.87	2.36	2.67	5.23	11.13	4.81
32-4		0.10	0.51	0.70	1.32	0.47	1.41	1.44	2.92	6.24	4.72
32-5		0.43	2.63	3.07	6.14	2.12	6.57	7.07	13.30	29.07	4.73
32-6		0.08	0.31	0.56	1.02	0.35	0.91	0.94	1.82	4.03	3.94

Table 16 (Continued)

Position-Particle	Batch	Quantity of Gas (n moles)									
		^{83}Kr	^{84}Kr	^{86}Kr	Σ Kr	^{131}Xe	^{132}Xe	^{134}Xe	^{136}Xe	Σ Xe	Xe/Kr
33-1	A-762	0.61	4.07	5.31	9.99	3.45	11.51	12.11	23.28	50.35	5.04
33-2		0.49	3.44	4.41	8.35	2.73	9.70	10.11	19.78	42.32	5.07
33-3		0.02	0.07	0.07	0.16	0.05	0.12	0.16	0.28	0.61	3.81
33-4		0.57	3.64	4.72	8.92	3.07	10.61	10.96	21.42	46.06	5.16
33-5		0.47	3.25	4.00	7.73	2.80	9.45	9.95	19.17	41.36	5.35
33-6		0.57	4.11	4.89	9.57	3.37	11.52	12.44	24.06	51.39	5.37
35-1	A-782	0.53	3.41	4.09	8.04	2.92	9.83	10.46	20.32	43.53	5.41
35-2		0.54	3.41	4.20	8.15	2.86	9.54	10.13	20.27	42.80	5.25
35-3		0.54	3.36	4.34	8.24	2.71	9.45	9.88	19.62	41.66	5.06
35-4		0.50	3.39	4.19	8.09	2.93	9.82	10.15	19.98	42.88	5.30
35-5		0.39	2.73	3.30	6.43	2.21	7.57	7.99	15.32	33.10	5.15
35-6		0.42	2.84	3.52	6.79	2.35	8.31	8.52	16.39	35.58	5.24
36-1	A-786	0.56	3.56	4.69	8.81	3.11	10.49	10.75	21.02	45.38	5.15
36-2		0.48	3.39	4.13	8.01	2.79	9.53	9.77	19.10	41.19	5.14
36-3		0.47	3.33	3.85	7.65	2.80	9.49	9.93	19.42	41.65	5.45
36-4		0.62	3.93	4.55	9.09	3.32	11.18	12.03	23.03	49.56	5.45
36-5		0.67	4.22	5.25	10.14	3.58	12.59	13.42	26.10	55.69	5.49
36-6		0.49	3.46	4.28	8.23	2.76	9.85	9.95	19.51	42.08	5.11
38-1	A-787	0.53	3.11	3.90	7.55	2.84	9.69	10.41	20.47	43.41	5.75
38-2		0.59	3.70	4.75	9.04	3.34	11.32	12.13	23.63	50.42	5.57
38-3		0.25	1.30	1.73	3.28	1.28	3.59	4.18	8.10	17.15	5.23
38-4		0.53	3.35	4.31	8.19	3.12	10.33	11.02	21.56	46.03	5.61
38-5		0.57	3.50	4.52	8.60	2.96	10.19	10.85	21.28	45.29	5.26
38-6		0.59	3.62	4.64	8.84	3.29	10.96	12.13	23.49	49.89	5.64
39-1-1	OR-1975-T	0.42	2.92	3.88	7.22	2.33	8.14	8.20	15.91	34.58	4.79
39-1-2		0.65	3.91	5.17	9.73	3.30	11.29	11.84	23.10	49.53	5.09

Table 16 (Continued)

Position-Particle	Batch	Quantity of Gas (n moles)									
		^{83}Kr	^{84}Kr	^{86}Kr	Σ Kr	^{131}Xe	^{132}Xe	^{134}Xe	^{136}Xe	Σ Xe	Xe/Kr
39-1-3		0.49	3.26	4.33	8.09	2.64	9.35	9.35	18.14	39.49	4.88
39-1-4		0.41	2.94	3.91	7.26	2.31	8.19	8.13	15.90	34.53	4.75
39-1-5		0.51	3.46	4.58	8.55	2.64	9.67	9.62	18.90	40.83	4.78
39-1-6		0.53	3.58	4.75	8.87	2.98	10.20	10.76	21.08	45.03	5.08
39-2-1	OR-2013-T	0.47	3.15	3.63	7.25	2.37	8.16	8.26	16.48	35.27	4.86
39-2-2		0.09	0.34	0.56	0.99	0.30	0.62	0.87	1.66	3.46	3.47
39-2-3		0.54	3.56	4.58	8.68	2.87	9.68	9.94	19.70	42.20	4.86
39-2-4		0.14	0.45	0.75	1.34	0.43	0.89	1.27	2.56	5.15	3.84
39-2-5		0.68	4.29	5.47	10.45	3.61	12.44	13.11	25.46	54.63	5.23
39-2-6		0.57	3.84	5.04	9.46	3.19	10.91	10.92	21.63	46.65	4.93
		Low-temperature Magazine									
40-1	A-765	0.28	1.23	1.74	3.25	1.03	3.41	3.61	7.38	15.43	4.73
40-2		0.42	2.36	3.13	5.91	1.91	6.29	6.92	13.70	28.82	4.88
40-3		0.16	0.98	1.28	2.43	0.80	2.70	2.86	5.73	12.09	4.98
40-4		0.31	2.03	2.60	4.94	1.70	5.44	5.77	11.28	24.20	4.89
40-5		0.42	2.59	3.34	6.36	2.19	7.10	7.76	15.07	32.13	5.05
40-6		0.38	1.98	2.55	4.91	1.62	5.66	5.95	11.88	25.12	5.12
42-1	A-780	0.40	2.22	2.84	5.45	1.72	5.37	5.90	11.60	24.58	4.51
42-2		0.41	2.06	2.64	5.12	1.56	5.27	5.65	11.34	23.83	4.65
42-3		0.35	1.91	2.48	4.74	1.49	4.65	5.08	10.15	21.38	
42-4		0.48	2.35	3.23	6.07	1.83	6.11	6.64	13.20	27.77	
42-5		0.43	2.00	2.61	5.05	1.52	5.07	5.75	11.16	23.49	
42-6		0.46	2.02	2.90	5.38	1.58	5.25	5.68	11.34	23.85	

Table 16 (Continued)

Position-Particle	Batch	Quantity of Gas (n moles)									
		^{83}Kr	^{84}Kr	^{86}Kr	Σ Kr	^{131}Xe	^{132}Xe	^{134}Xe	^{136}Xe	Σ Xe	Xe/Kr
43-1	A-785	0.38	1.96	2.50	4.83	1.54	5.80	5.46	10.92	23.00	4.76
43-2		0.40	1.92	2.48	4.80	1.65	4.91	5.40	10.63	22.60	4.71
43-3		0.40	2.08	2.72	5.20	1.67	5.41	5.87	11.60	24.55	4.72
43-4		0.09	0.52	0.76	1.38	0.44	1.50	1.57	3.23	6.74	4.89
43-5		0.38	2.03	2.58	5.00	1.60	5.12	5.63	11.22	23.57	4.72
43-6		0.13	0.74	1.00	1.88	0.59	1.93	2.07	4.31	8.90	4.73
45-1	A-806	0.14	0.78	1.02	1.94	0.61	1.99	2.08	4.39	9.08	4.68
45-2		0.37	2.09	2.64	5.10	1.73	5.32	5.93	11.61	24.61	4.82
45-3		0.39	1.91	2.48	4.78	1.49	4.85	5.03	10.61	21.34	4.46
45-4		0.13	0.71	0.97	1.81	0.61	1.93	2.01	4.20	8.75	4.82
45-5		0.15	0.88	1.20	2.23	0.73	2.38	2.52	5.18	10.81	4.84
45-6		0.39	2.00	2.57	4.96	1.69	5.05	5.72	11.27	23.73	4.78
46-1	A-762	0.32	1.52	1.88	3.72	1.38	4.26	4.74	9.55	19.93	5.35
46-2		0.32	1.59	2.01	3.92	1.54	4.39	4.88	9.75	20.57	5.25
46-3		0.32	1.62	2.07	4.02	1.40	4.35	4.78	9.51	20.04	4.98
46-4		0.31	1.51	1.95	3.78	1.42	4.42	4.88	9.65	20.36	5.39
46-5		0.28	1.33	1.79	3.41	1.17	3.84	4.17	8.52	17.71	5.19
46-6		0.12	0.60	0.83	1.56	0.48	1.53	1.70	3.53	7.25	4.65
48-1	A-782	0.08	0.23	0.40	0.71	0.24	0.66	0.76	1.61	3.28	4.60
48-2		0.27	1.23	1.65	3.15	1.04	3.07	3.32	6.80	14.23	4.51
48-3		0.36	1.59	2.02	3.97	1.26	3.73	4.16	8.33	17.48	4.40
48-4		0.31	1.47	1.82	3.61	1.20	3.61	4.01	8.08	16.90	4.68
48-5		0.29	1.40	1.79	3.48	1.09	3.26	3.70	7.29	15.35	4.41
48-6		0.56	2.89	1.47	4.92	2.74	5.17	8.08	13.24	29.24	5.94

Table 16 (Continued)

Position-Particle	Batch	Quantity of Gas (n moles)									
		^{83}Kr	^{84}Kr	^{86}Kr	Σ Kr	^{131}Xe	^{132}Xe	^{134}Xe	^{136}Xe	Σ Xe	Xe/Kr
49-1	A-786	0.05	0.25	0.46	0.76	0.22	0.71	0.68	1.55	3.15	4.16
49-2		0.22	0.74	1.08	2.05	0.65	1.89	2.14	4.38	9.06	4.43
49-3		0.29	1.32	1.85	3.46	1.02	3.14	3.47	7.06	14.70	4.24
49-4		0.45	1.91	2.58	4.94	1.39	4.36	4.73	9.72	20.20	4.09
49-5		0.36	1.25	1.78	3.40	0.99	3.18	3.37	6.98	14.52	4.27
49-6		0.16	0.70	0.94	1.80	0.57	1.69	1.92	3.90	8.09	4.49
52-1	OR-1975-T	0.09	0.46	0.66	1.22	0.37	1.02	1.26	2.65	5.36	4.40
52-2		0.08	0.36	0.56	1.01	0.32	0.86	0.92	2.09	4.25	4.21
52-3		0.19	0.60	0.96	1.75	0.56	1.60	1.79	3.79	7.74	4.41
52-4		0.03	0.15	0.23	0.42	0.14	0.35	0.39	0.81	1.69	4.05
52-5		0.12	0.43	0.70	1.24	0.34	1.09	1.22	2.64	5.28	4.24
52-6		0.06	0.21	0.37	0.64	0.19	0.59	0.63	1.41	2.82	4.40

Table 17. Summary of Condition of Biso Coatings from HT-34 as Determined by PGA System

Batch	Magazine[a]	
	High Temperature	Low Temperature
A-765	P_1; T_5	P_2; T_4
A-780	T_6	T_6
A-785	T_6	P_2; T_4
A-806	P_6	P_3; T_3
A-762	P_1; T_5	P_1; T_5
A-782	T_6	P_1; T_5
A-786	T_6	P_2; T_4
A-787	P_1; T_5	*b*
OR-1975-T	T_6	P_2; T_4
OR-2013-T	P_2; T_4	*c*

[a] T = gastight; P = permeable; subscript denotes number of particles.

[b] Particles not available.

[c] Not included in low-temperature magazine.

Also worthy of note are two of the six particles from batch OR-2013-T that became permeable. These two particles are from the batch of CO_2-diluent coatings that appeared to demonstrate excellent performance in capsules HT-18 and HT-19,[3] as indicated from the visual appearance of the particles and the gas-content measurements of five particles. Although there was scatter in the gas-content data obtained with an earlier version of a gas analyzer, the particles were judged to be gastight at the time.

The yields of krypton and xenon in the HT-34 particles were calculated using data acquired with the IMGA system,[12] CACA-2 (ref. 9), and a modified version of the CACA-2 code.[8] The theoretical fission-gas content of the individual particles was based on the ^{95}Zr present, as determined by IMGA after correcting for ^{154}Eu. Because the experiment was removed from HFIR on November 23, 1977, less than 1% of the ^{95}Zr

remained at the time the gamma analyses were made. Although a live counting time of 500 s was used, there were counting errors up to 16%. These errors will not detract from the ability to detect permeable coatings, but there is an obvious need to improve the precision of the measurements.

To accomplish this, additional fission-gas inventory calculations will be determined based on ^{106}Ru, which has a 369-d half-life in contrast to 65 d for ^{95}Zr. The ^{106}Ru activity, measured by IMGA, will be used to determine the number of fissions occurring for each particle examined. This number, together with an appropriate fission product yield for the HFIR Target Facility, will be used to calculate the amount of specific fission product isotopes present at end-of-life. For the fission-gas inventory present, the ^{86}Kr isotope is of major interest because its source is primarily from fission. It also has a relatively low capture cross section so that loss corrections due to (n,γ) reactions are insignificant. The measured PGA concentration of ^{86}Kr can then be compared with the calculated value to assess fission-gas retention. This work is currently under way, and the results will be presented in a future report.

Because the IMGA data are currently being reanalyzed for inclusion in another report,[13] the fission gas released from particles at breakage was compared with calculated quantities determined by using the calculated burnup values reported in Table 7. The calculated burnups were used in conjunction with mean kernel diameters, a fission-gas yield of 0.3, and a density of 9.9 Mg/m^3 for ThO_2 kernels to calculate the moles of fission gas generated in individual particles for each of the positions in HT-34 that contained loose ORNL Biso particles. The total quantities of fission gases released at particle breakage were corrected for the ^{85}Kr not measured by the PGA system (Σ Xe + Σ Kr/0.92) and compared with the calculated quantity of fission gas expected for each ORNL holder position (Fig. 10). Separation of the gastight particles from the permeable particles is highly apparent in Fig. 10 and shows, as in Table 17, that particles from only one batch (A-780) remained gastight in both the high- and low-temperature positions. Note that two particles from batches A-762 and A-765 from the high-temperature magazine showed essentially zero release of fission gas at particle breakage. This indicates that

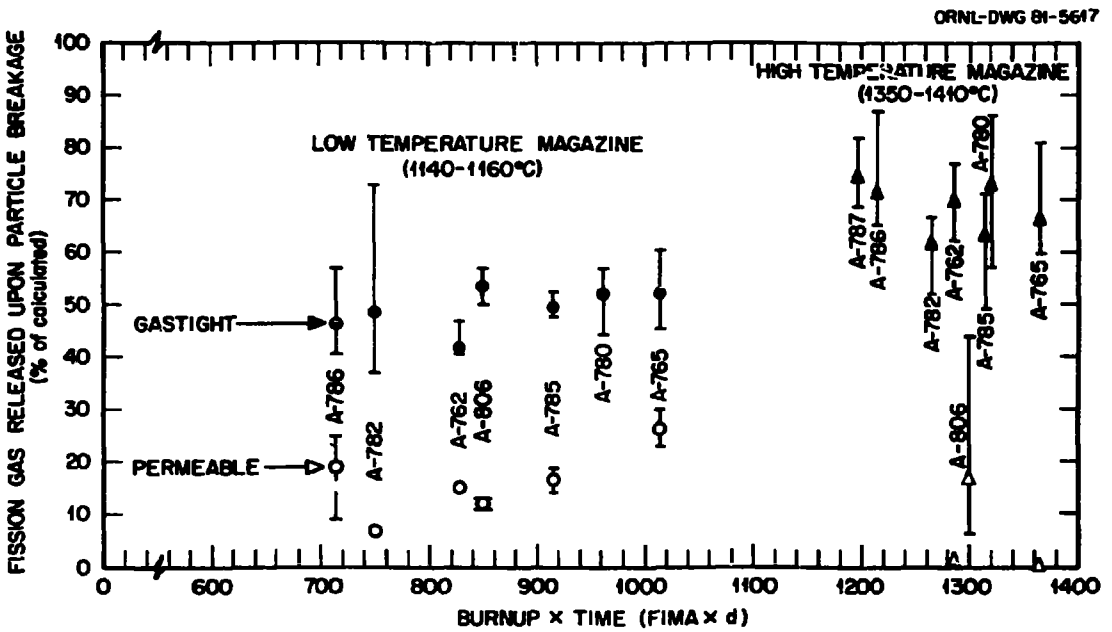

Fig. 10. Correlation of Fission Gas Released Upon Particle Breakage with Burnup and Time for Loose Biso-coated Particles in Capsule HT-34. Only particles from batch A-780 remained gastight in both the high- and low-temperature magazines.

there is not enough fission-gas release associated with kernel breakage to influence the determination of gastight vs permeable coatings.

The quantity of fission gas (FG) expected to be released from the ThO_2 kernels was determined from the following relationship:[14]

$$\text{FG release (\%)} = 34.9e^{-\frac{1378}{T}\left(1+\frac{3.34}{f}\right)t^{0.237}},$$

where:

T = time-averaged temperature (K),

f = burnup (% FIMA), and

t = time (h).

Results for the particles judged to be gastight (Fig. 10) were compared with the calculated release values from the kernel. As shown in Fig. 11, there is good correlation between the measured and calculated release values. Apparently, the calculated release values are slightly

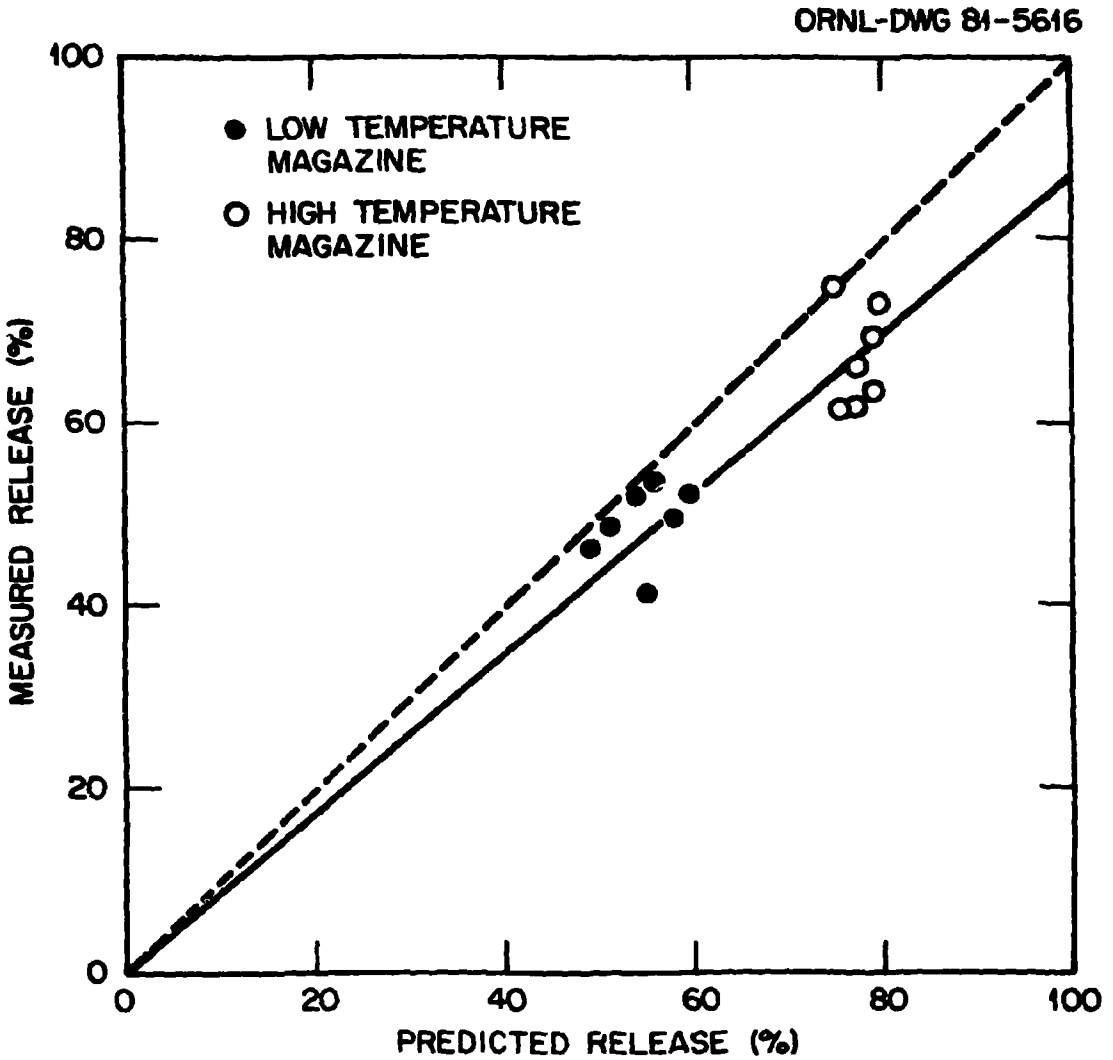

Fig. 11. Correlation of Predicted Release with Measured Release of Fission Gas from Gastight Biso-coated ThO_2 Particles in Capsule HT-34. The dashed line represents a perfect fit.

high; however, it should be emphasized that gas-release measurements were made at room temperature. In the future we plan to make similar measurements at temperatures approximating the irradiation temperature; an increase in release is expected.

INERT-GAS-INTRUSION MEASUREMENTS

The behavior of pyrocarbon coatings during irradiation is of prime importance in the behavior of Biso fuel particles. A key question is will fission gases be released from the fuel because of radiation-induced permeability? In this work, the permeability of irradiated pyrocarbon coatings was determined for several batches of fuel particles in which the high-density pyrocarbon coatings were deposited on inert (carbon) kernels. The procedure for determining permeability of Biso coatings has been reported.[15] The high radioactivity of irradiated particles with thorium- and uranium-containing kernels made it impossible to obtain neon-helium permeability measurements because of the mass spectrometer location. Results of measurements on particles with inert kernels clearly demonstrate that inert-gas permeability of the pyrocarbon coatings decreases with increasing neutron fluence, at least to a fluence as high as 10.2×10^{25} n/m^2 (>0.18 MeV). These data are shown in Table 18 for inert kernel particle batches tested in irradiation experiment HT-34. In each irradiation position neon-helium permeability decreased with increasing neutron fluence. In the last column of Table 18 neon-helium permeability is given as a percentage of the unirradiated permeability; permeability decreased 72% in the most severe case (28% of the original).

Fission products and gas pressure could affect the behavior of fuel particle coatings with uranium- or thorium-containing kernels, but the results of our work with inert kernels clearly demonstrate that disorder created by neutron damage does not cause the pyrocarbon coatings to become more permeable to inert gases.

CONCLUSIONS

The primary objective of this experiment was to investigate the influence of variations in coating conditions on the irradiation performance of Biso- and Triso-coated ThO_2 particles. In the Biso-coated particles the LTI physical properties were varied, and in the preparation of Triso-coated particles SiC deposition rates were varied.

Table 18. Pyrocarbon Coating Permeability of Inert Biso Particles Irradiated in HT-34

Particle Batch	Specimen Designation	Neutron Fluence >0.18 MeV (n/m^2)	Design Irradiation Temperature (°C)	Gas Uptake per Particle (pmol)		Ne/He Ratio	Ne/He Ratio (% of Preirradiation Ratio)
				He	Ne		
OR-2722-1-H		0		81	24	0.29	
OR-2722-1-H	28-3 Top	4.8×10^{25}	900	101	13	0.15	52
OR-2722-1-H	26-3 Top	9.1	1250	114	15	0.11	28
OR-2725-1-H		0		84	26	0.31	
OR-2725-1-H	28-3 Bottom	4.8	900	126	15	0.12	39
OR-2725-1-H	26-3 Bottom	9.1	1250	125	14	0.11	36
OR-2730-1-H		0		117	35	0.30	
OR-2730-1-H	28-1	8.2	900	149	36	0.24	80
OR-2730-1-H	26-1	10.2	1250	165	28	0.17	57

Visual examination of the Biso-coated particles after irradiation showed that in the low-temperature magazine a significant number of particles from all batches except one failed. In the high-temperature magazine particles from three of the eight A batches, which were prepared in the 0.13-m coating furnace, showed no failures. All failures were a result of pressure-vessel failure, and no correlation could be made between physical property data and failure frequency. However, in checking the fabrication history of the particles prepared in the 0.13-m coating furnace, it was determined that the particles had not received a post-coating anneal. This is probably the reason for the lower number of failures in the high-temperature magazine (i.e., the LTIs were partially stress relieved in the reactor). (Samples of particles from six of the eight A batches were subsequently annealed at 1800°C for 30 min and included in capsule HRB-14; they are currently being examined.)

Measurement of the quantities of fission gases released at individual particle breakage at room temperature in the PGA system showed that only particles from batch A-780 remained gastight in both the high- and low-temperature magazines. There were particle samples from four of the eight A batches that remained gastight in the high-temperature magazine. Similarily, as in the case of the visual examination results, the higher survival frequency in the high-temperature magazine is probably associated with in-reactor stress relieving of the LTI. Apparently, there was considerable variation in the coating properties within the batches of particles. There was only one instance in which all the particles in a sample were permeable; typically, three to five particles in a sample of six would be gastight.

Visual examination of the particles from the two small-coater batches of Biso particles (OR-1975-T and OR-2013-T) that had received a post-coating anneal confirmed the earlier results from the HT-19 experiments. In HT-34 no failures occurred in the particles from batch OR-2013-T (CO_2-diluent LTI), and between 14 and 24% of the particles from OR-1975-T failed as a result of fast-neutron damage. More than 90% of the particles from OR-1975-T failed from fast-neutron damage in HT-19, but they reached a flux level 140% greater than that experienced in HT-34.

Although no failures were observed for the particles from OR-2013-T in HT-34, measurement of the fission-gas content with the PGA system showed that one-third of the coatings became permeable during irradiation.

Gamma analyses of individual Biso-coated ThO_2 particles with the IMGA system showed that the particles in the low-temperature magazine retained all their ^{137}Cs, but the particles in the high-temperature magazine lost between 55 and 85% of the ^{137}Cs produced. Gamma analyses of the Triso-coated ThO_2 particles showed that, based on ^{137}Cs retention, of the four SiC deposition rates used (0.16 to 0.45 μm/min), the best performer at the higher temperatures and burnups was the SiC deposited at the highest rate. Admittedly, this apparent trend must be tempered by the fact that considerations other than deposition rate alone could have significantly affected these results. Detailed characterization studies, which should be performed to quantify the performance of these SiC coatings, is beyond the scope of this experiment.

Inert-gas-intrusion measurements on the Biso-coated inert (carbon) particles from three batches consistently showed significant decreases in permeability, ranging from about 20 to 72% after irradiation. These results could suggest that volatile fission products and high internal gas pressures in uranium- or thorium-bearing fuel particles affect the integrity of LTI coatings and that results obtained on inert particles cannot be translated to fuel particle performance.

ACKNOWLEDGMENTS

The authors acknowledge the efforts of many people who made significant contributions to the planning, execution, and evaluation of this experiment: W. P. Eatherly and F. J. Homan for numerous discussions and essential support during the entire experiment; D. P. Stinton and B. A. Thiele of KFA Jülich for help in the planning; D. P. Stinton, G. W. Weber, B. R. Chilcoat, C. E. Devore, C. L. Garrison, and C. Hamby, Jr., for fabricating and characterizing the test particles; M. D. Allen for preirradiation metallography; W. J. Mason for preirradiation radiography; R. L. Hammer and B. R. Chilcoat for fabricating and characterizing the

fuel rod specimens; W. F. Rogers and H. A. Parker of the Analytical Chemistry Division for the hot chlorine leach analyses; J. A. Conlin and K. R. Thoms of the Engineering Technology Division for the in-reactor operation of the capsule; A. M. Howard for assistance in performing the thermal analyses; and E. L. Ryan and the staff of the High-Radiation-Level Examination Laboratory for the postirradiation disassembly of the capsule, visual examination, and PGA measurements.

The authors also acknowledge the help of the many people who assisted considerably in the preparation of this report: R. L. Pearson of the Chemical Technology Division and W. J. Lackey of the Metals and Ceramics Division for their critical review, Shirley Napier for technical editing, and the Technical Publications Department for final preparation of the report.

REFERENCES

1. C. A. Young and C. S. Jones, *Pre- and Postirradiation Evaluation of TRISO ThO_2 Particles Irradiated in Capsule HT-34*, DOE Report GA-A15612, General Atomic Company, to be published.

2. W. J. Lackey, D. P. Stinton, and J. D. Sease, "Improved Gas Distributor for Coating High-Temperature Gas-Cooled Reactor Fuel Particles," *Nucl. Tech* 35: 227 (September 1977).

3. E. L. Long, Jr., et al., *Irradiation Performance of HTGR Biso Fertile Particles in HFIR Experiments HT-17, -18, and -19*, ORNL/TM-6414 (November 1978).

4. M. J. Kania and A. M. Howard, *HTCAP-1-A Program for Calculating Operating Temperatures in HFIR Target Irradiation Experiments*, ORNL/TM-7336 (June 1980).

5. M. J. Kania and K. H. Valentine, *The Irradiated Microsphere Gamma Analyzer (IMGA), An Integrated System for HTGR Coated Particle Fuel Performance Assessment*, ORNL-5606 (February 1980).

6. M. J. Kania, et al., *Irradiation Performance of HTGR Fertile Fuel in HFIR Target Capsules HT-12 through HT-15: Part 1*, ORNL/TM-5305 (February 1977).

7. K. H. Valentine and M. J. Kania, *IMGA Operating Manual*, ORNL/TM-6576 (August 1979).

8. A. M. Howard and T. N. Tiegs, unpublished work.

9. E. J. Allen, *CACA-2: Revised Version of CACA-A Heavy Isotope and Fission Product Concentration and Calculational Code for Experimental Irradiation Capsules*, ORNL/TM-5266 (February 1976).

10. T. N. Tiegs, *Analysis of ThO_2 Particle Fission Product Behavior by Gamma Spectrometry*, report in preparation.

11. J M Robbins, M. J. Kania, and E. L. Long, Jr., "A System for Measuring Fission-Gas Inventories of HTGR Fuel Particles," *Proc. 27th Conf. Remote Systems Tech., 1979 (ANS)*, pp. 241–245.

12. K. H. Valentine and E. L. Long, Jr., "Fuel Particle Inspection with the Irradiated Microsphere Gamma Analyzer," *Trans. Am. Nucl. Soc.* 22: 213–14 (1975).

13. M. J. Kania et al., *Final Report on PWS FD-12: Quantification of Irradiation-Inducted Permeability in Pyrocarbon Coatings*, KFA-ORNL Publication, in preparation.

14. Personal communication from B. F. Meyers, General Atomic Company.

15. C. S. Morgan, *Characterization of Pyrocarbon Coatings of HTGR Fuel Particles by Inert Gas Intrusion*, ORNL/TM-6819 (September 1979).

APPENDIX A

THERMAL HISTORIES OF PARTICLES, HOLDERS, AND FUEL RODS IRRADIATED IN HT-34

Table A1. Time-averaged Temperature of the Surface of Loose Biso-coated Particles Coated in a Large-Diameter (0.23-m) Coater

Position	Batch	Time-averaged Temperature (K)
27	A-765	1618
29	A-780	1683
30	A-785	1675
32	A-806	1674
33	A-762	1681
35	A-782	1655
36	A-786	1637
38	A-787	1632
40	A-765	1308
42	A-780	1434
43	A-785	1416
45	A-806	1415
46	A-762	1419
48	A-782	1385
49	A-786	1371
51	A-787	1349

HIGH-TEMPERATURE MAGAZINE

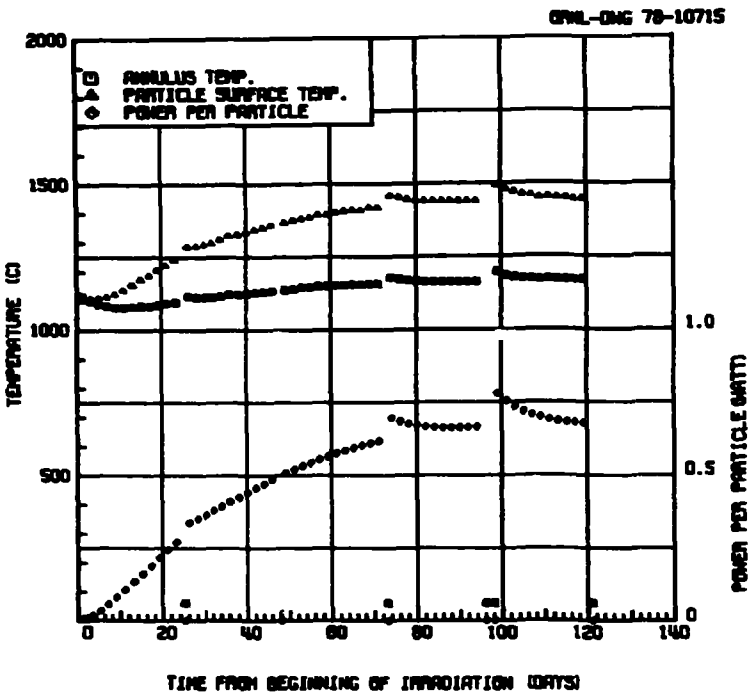

Particle Holder 27, Batch A-765

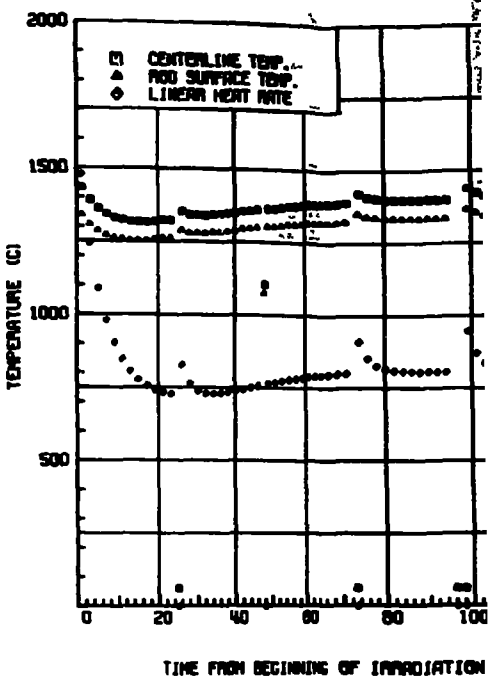

Fuel Rod Number 28, Batch A83

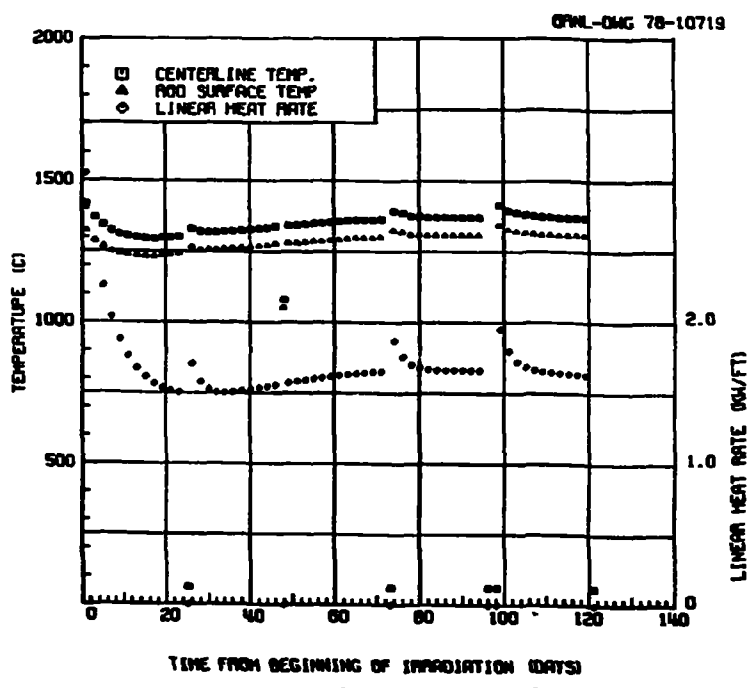

Fuel Rod Number 31, Batch A835+OR2576H

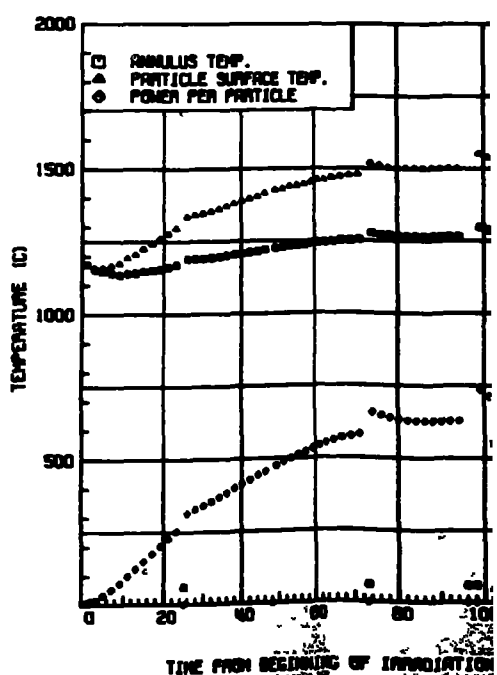

Particle Holder 32, Batc

Fig. A1. Temperature and Powe

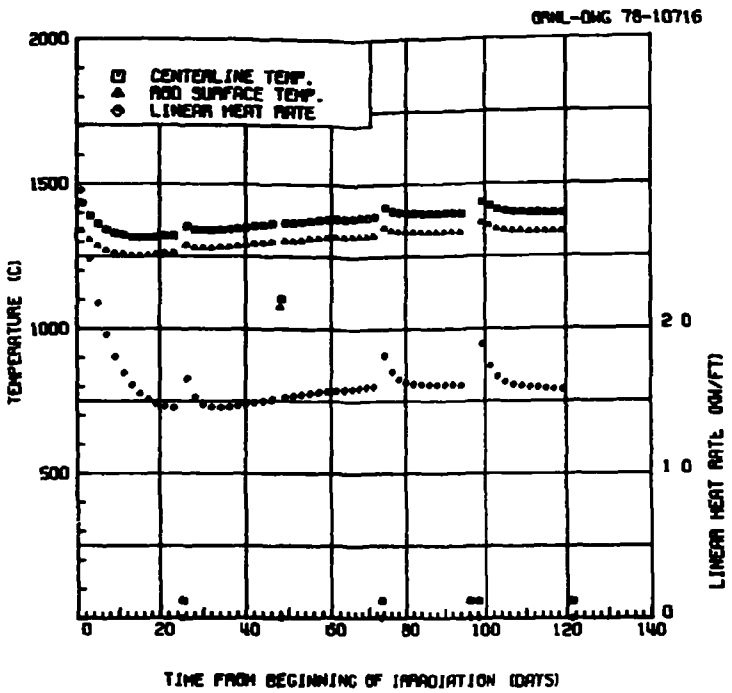

Fuel Rod Number 28, Batch A834 + OR-2576H

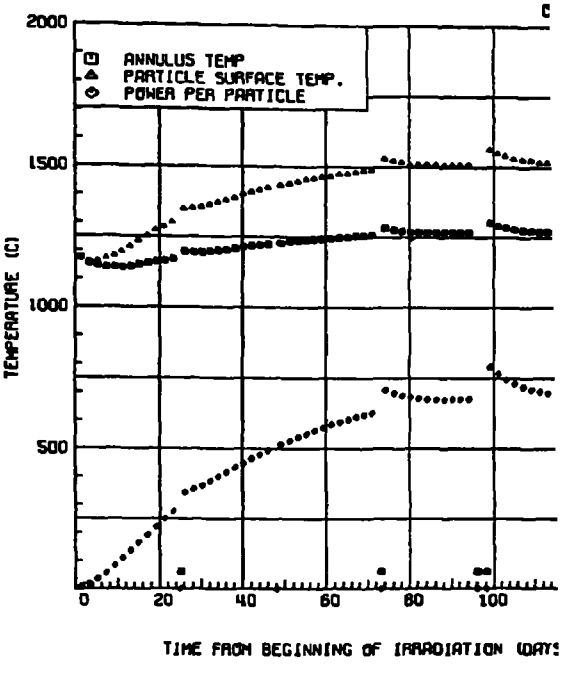

Particle Holder 29, Batch A-

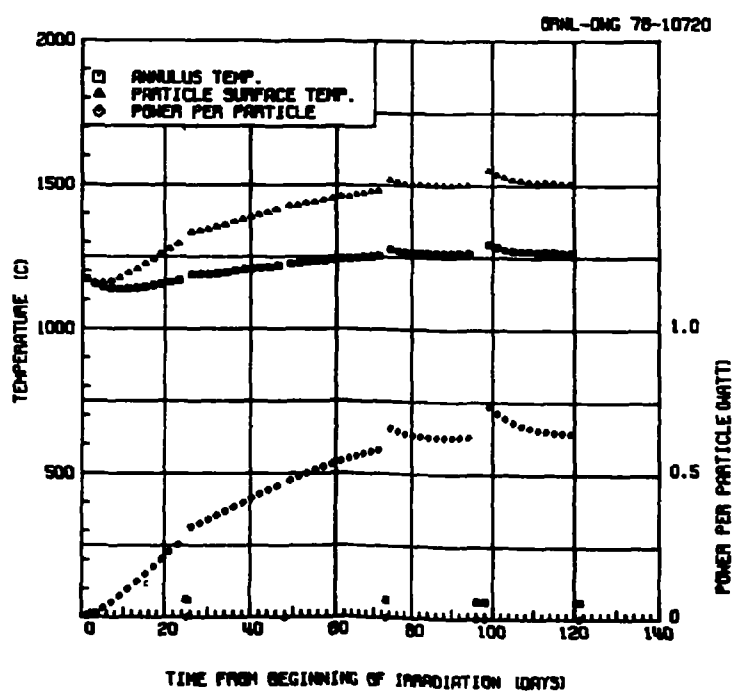

Particle Holder 32, Batch A-806

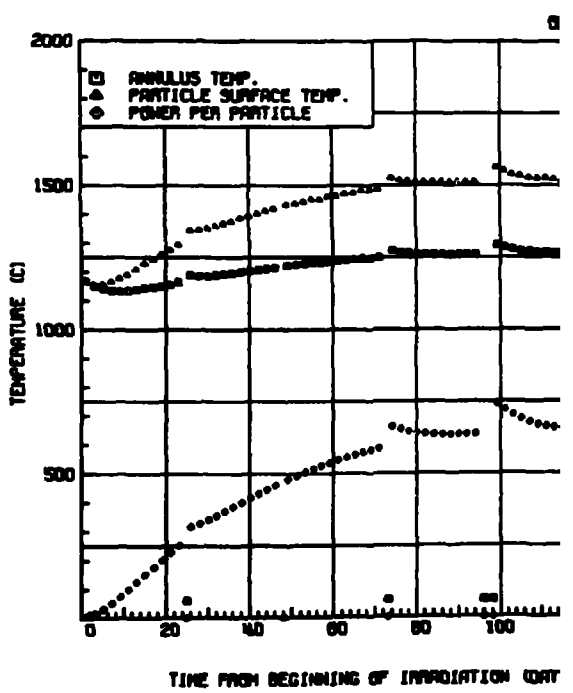

Particle Holder 33, Batch A

Fig. A1. Temperature and Power Histories for ORNL High Temperature Positions During Irradiati

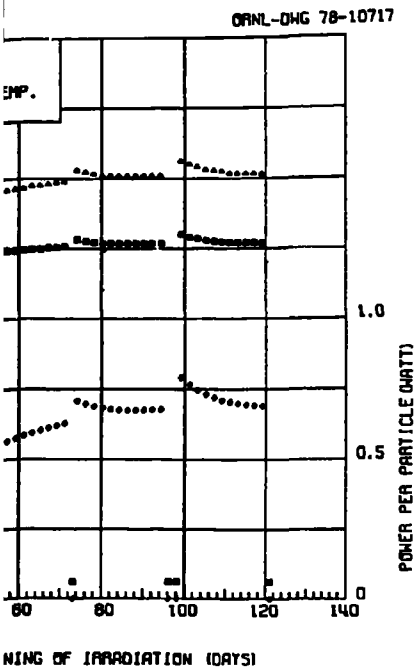

NING OF IRRADIATION (DAYS)

der 29, Batch A-780

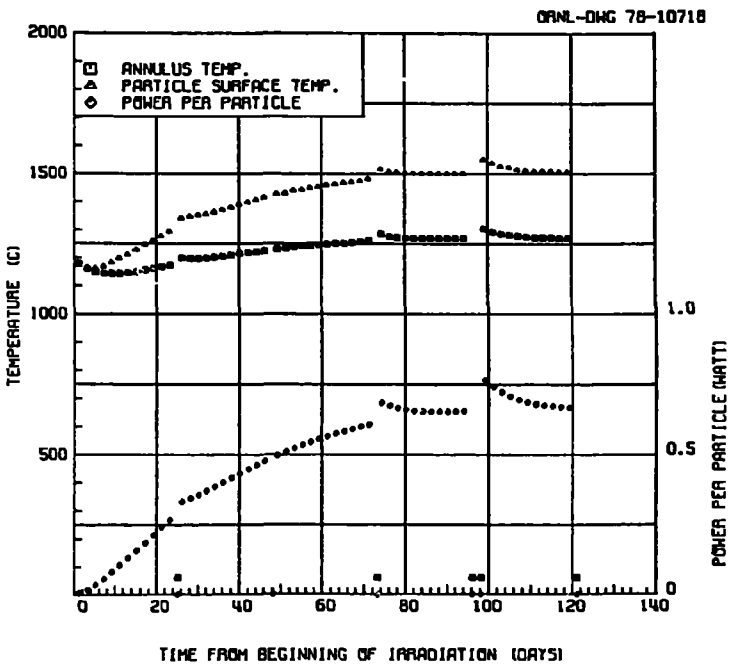

TIME FROM BEGINNING OF IRRADIATION (DAYS)

Particle Holder 30, Batch A-785

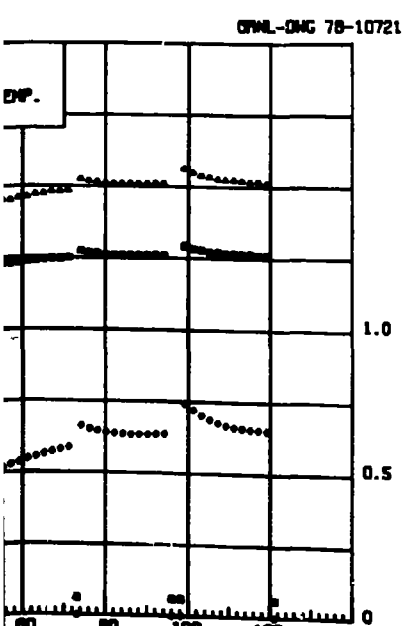

NING OF IRRADIATION (DAYS)

lder 33, Batch A-762

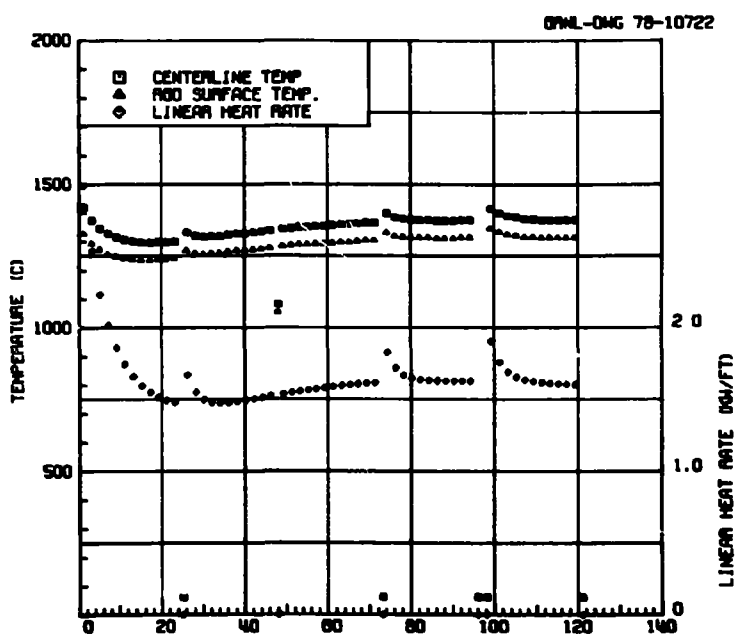

TIME FROM BEGINNING OF IRRADIATION (DAYS)

Fuel Rod Number 34, Batch A837+OR2576H

uring Irradiation in Capsule HT-34.

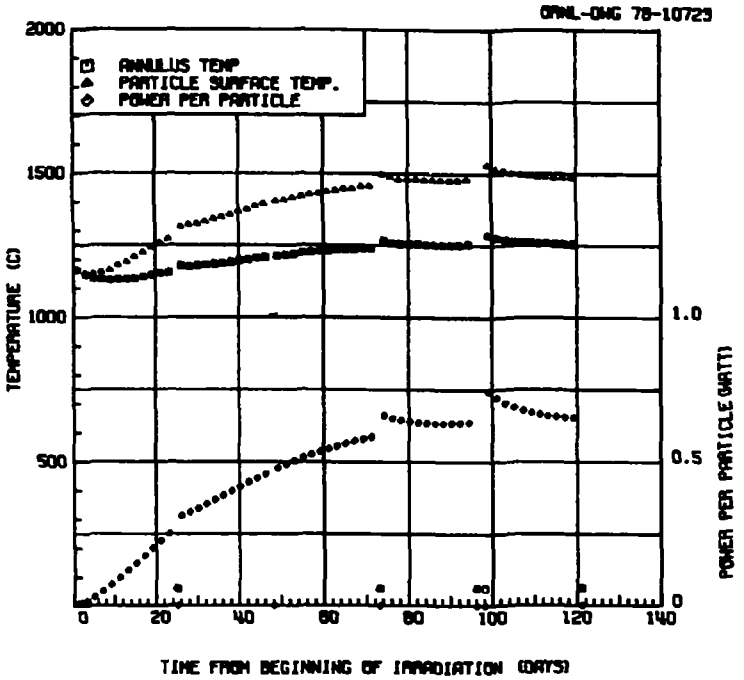

Particle Holder 35, Batch A-782

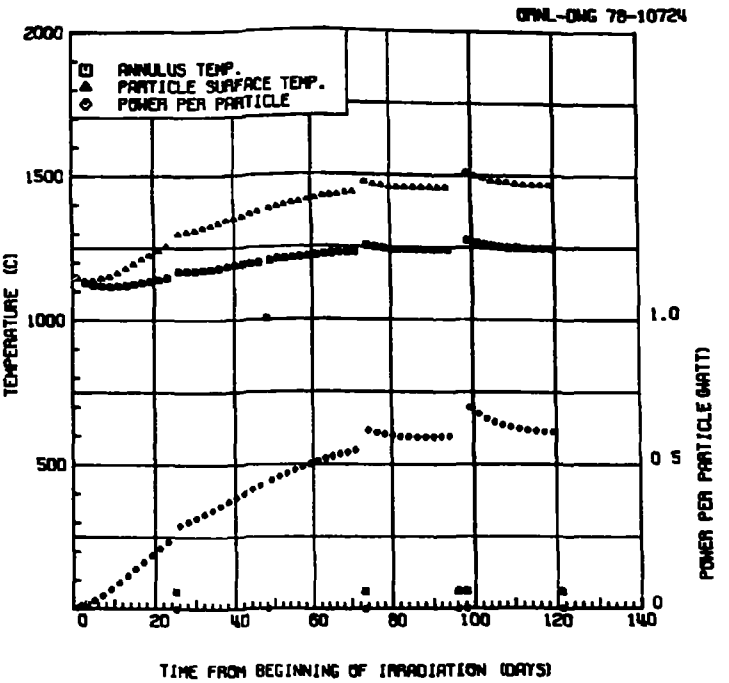

Particle Holder 36, Batch A-786

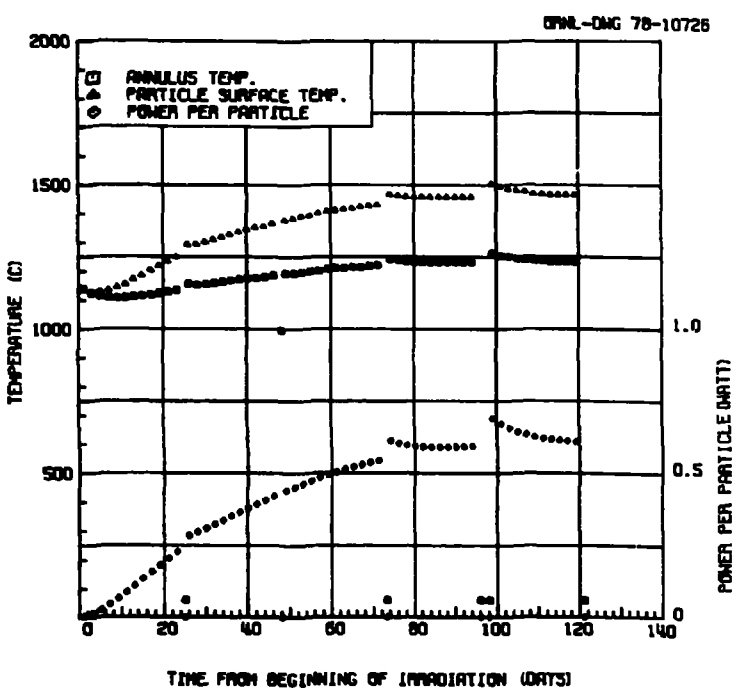

Particle Holder 38, Batch A-787

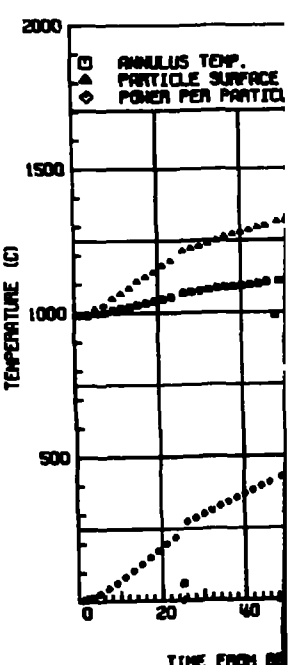

Particle Holde

Fig. A2. Temperature and Power Histories for ORNL High Temperature Positions Durin

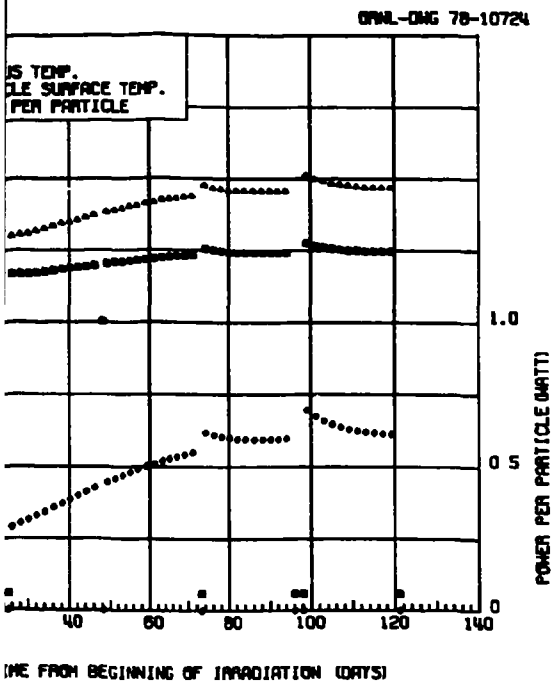

·ticle Holder 36, Batch A-786

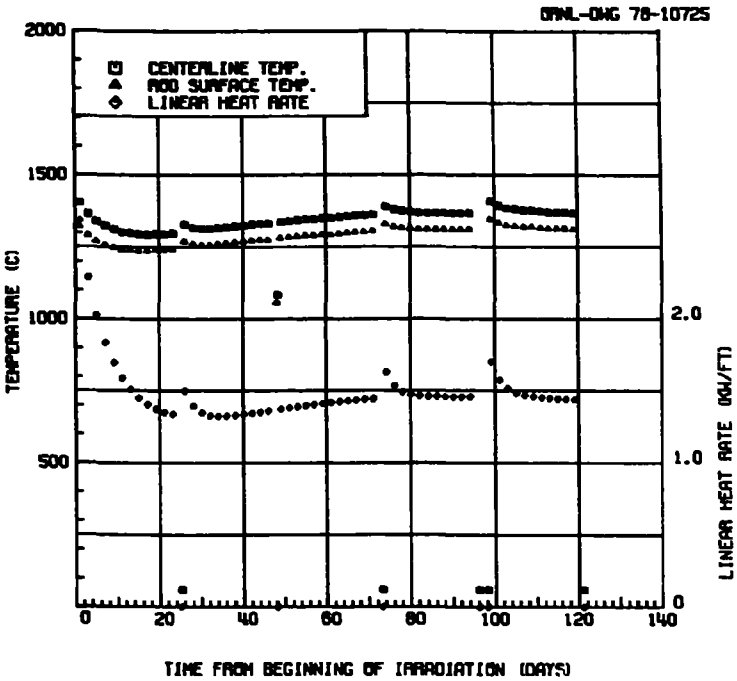

Fuel Rod Number 37, Batch A836+OR2576H

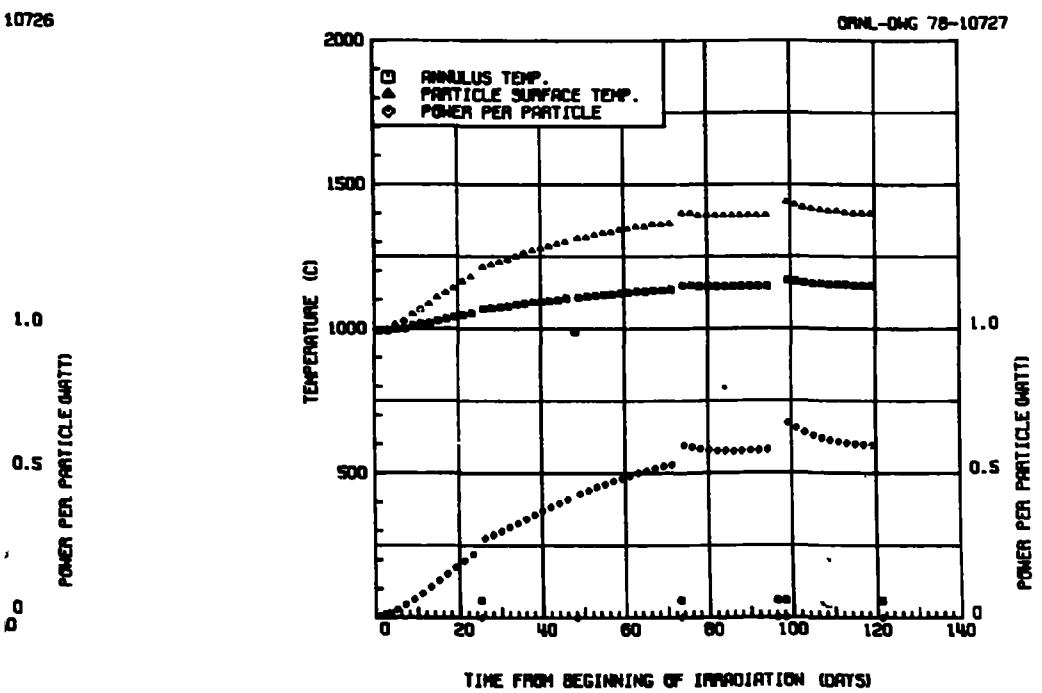

Particle Holder 39, Batch OR1925+OR2013T

ORNL High Temperature Positions During Irradiation in Capsule HT-34.

LOW-TEMPERATURE MAGAZINE

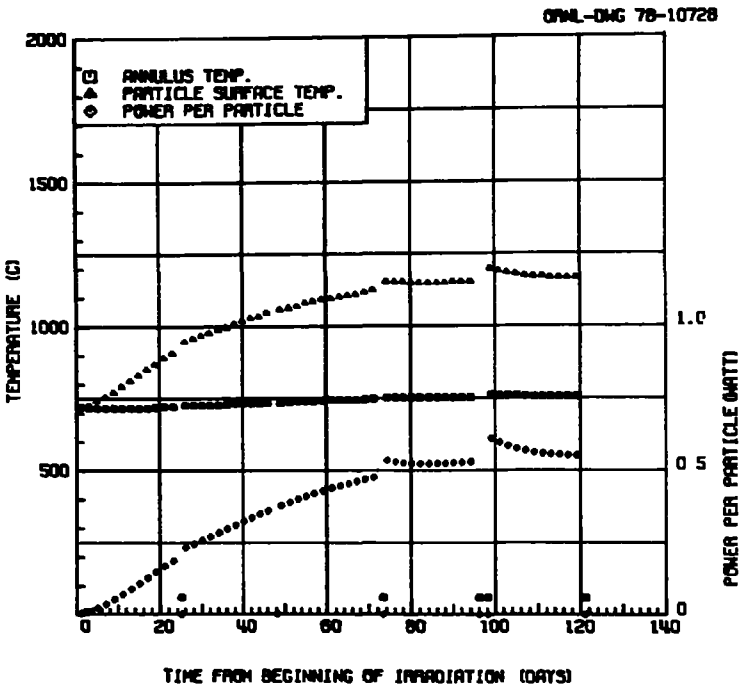

Particle Holder 40, Batch A-765

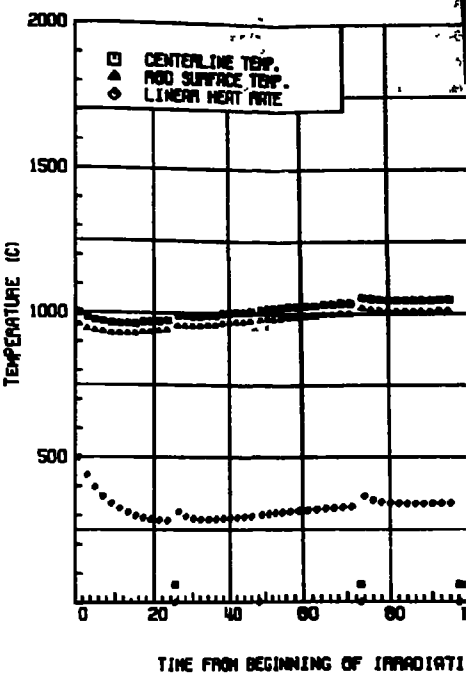

Fuel Rod Number 41, Batch

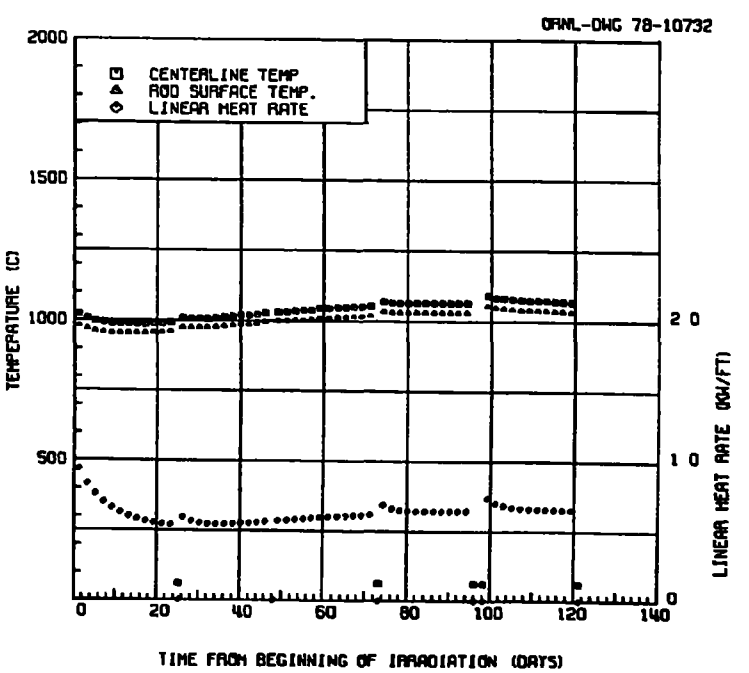

Fuel Rod Number 44, Batch A835+OR2576H

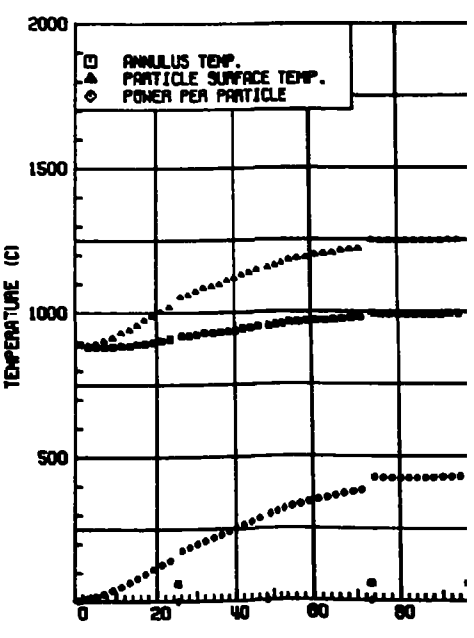

Particle Holder 45, Ba

Fig. A3. Temperature and Power His

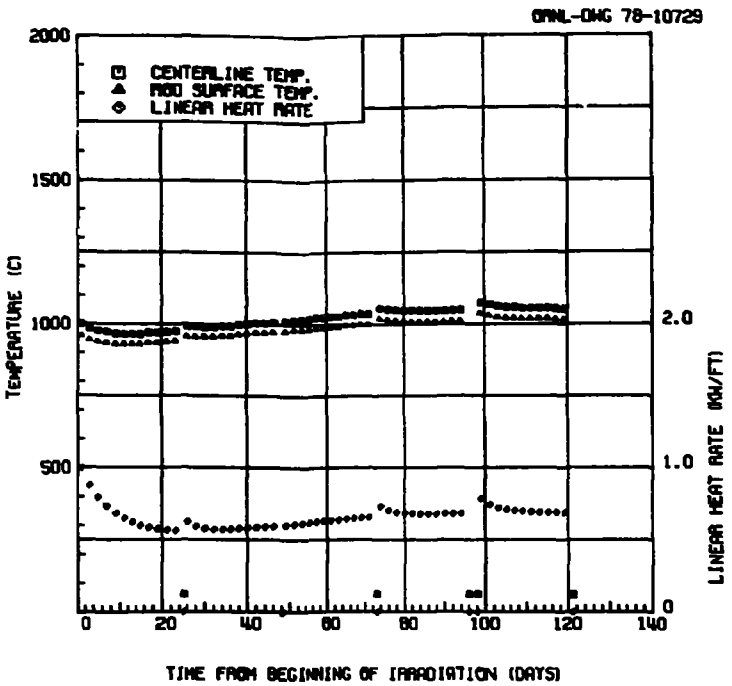

Fuel Rod Number 41, Batch A834+OR2576H

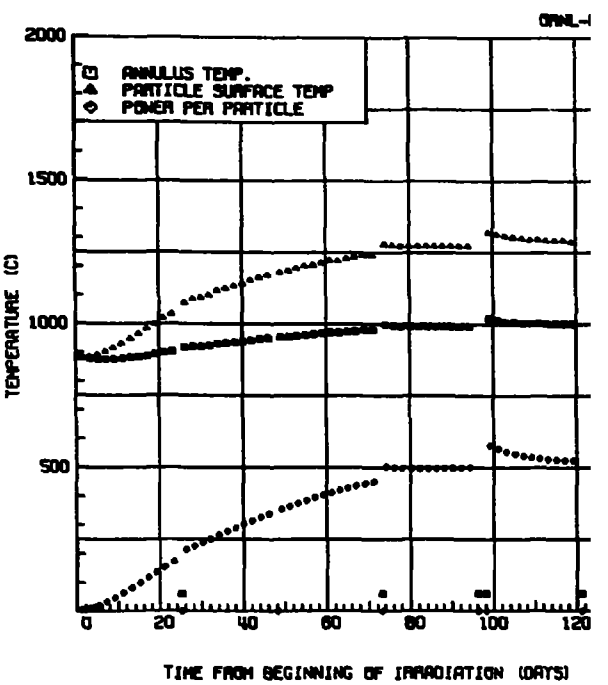

Particle Holder 42, Batch A-7

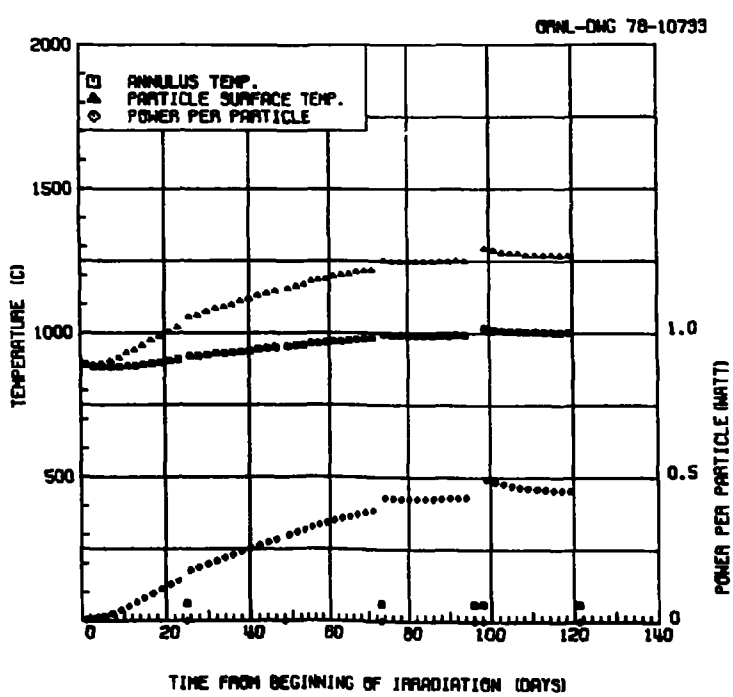

Particle Holder 45, Batch A-806

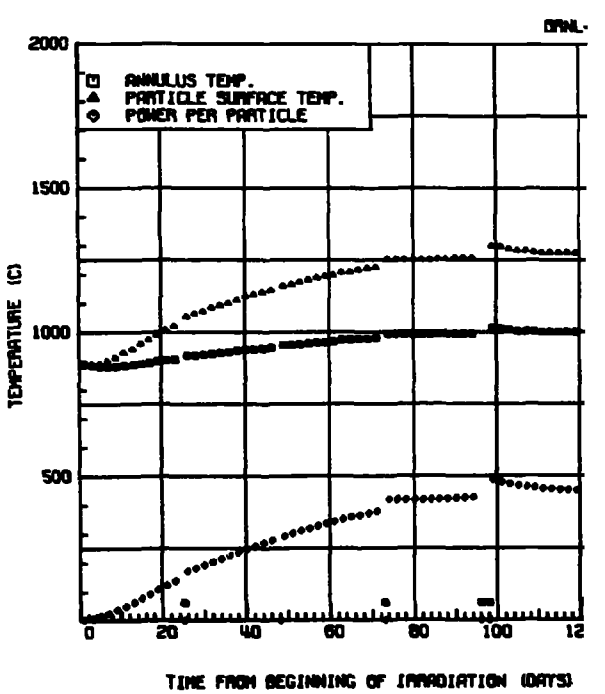

Particle Holder 46, Batch A-

Fig. A3. Temperature and Power Histories for ORNL Low Temperature Positions During Irradiation in Cap

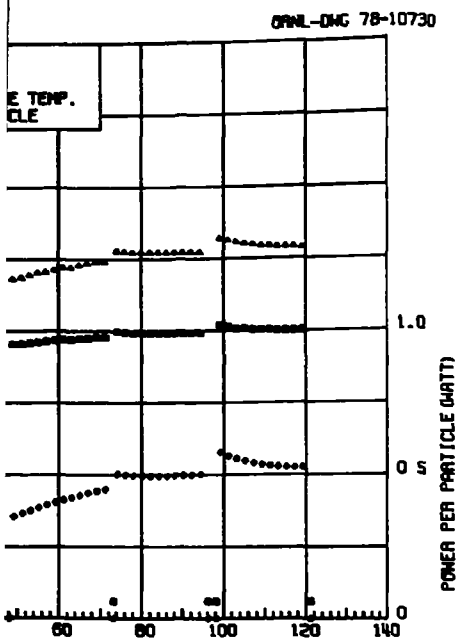

Holder 42, Batch A-780

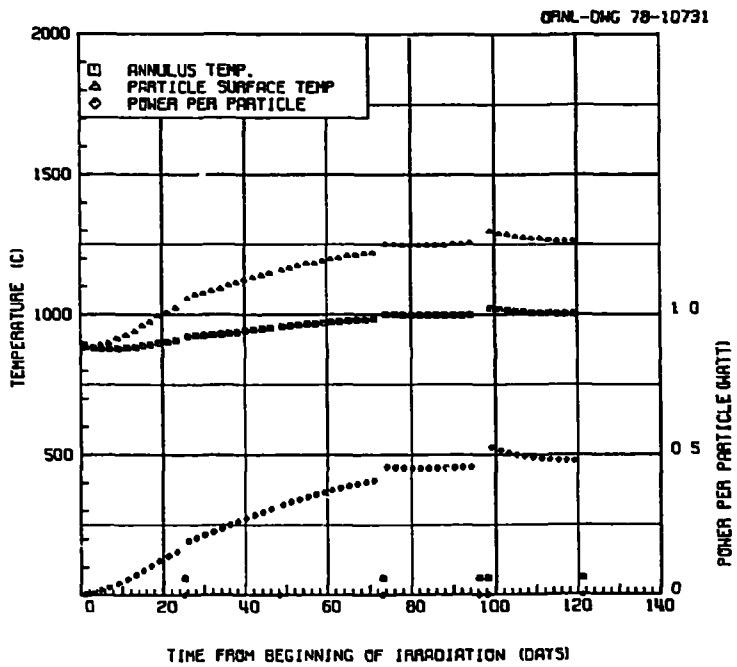

Particle Holder 43, Batch A-785

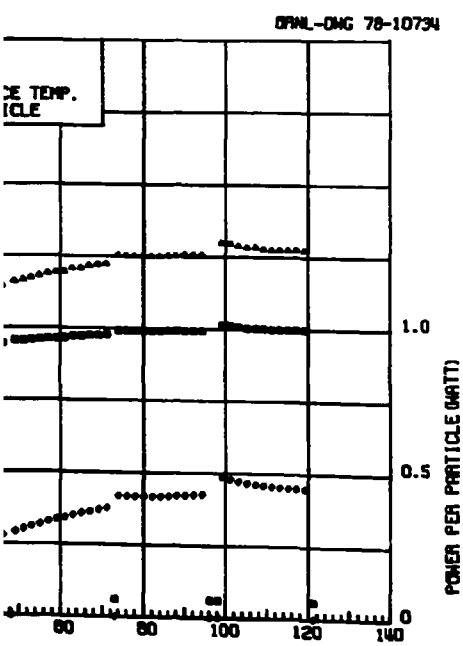

Holder 46, Batch A-762

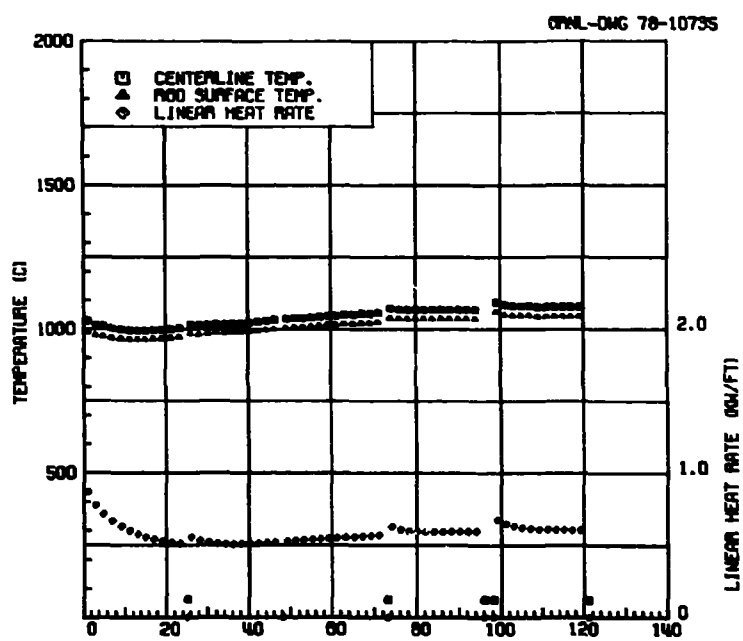

Fuel Rod Number 47, Batch A837+OR2576H

g Irradiation in Capsule HT-34.

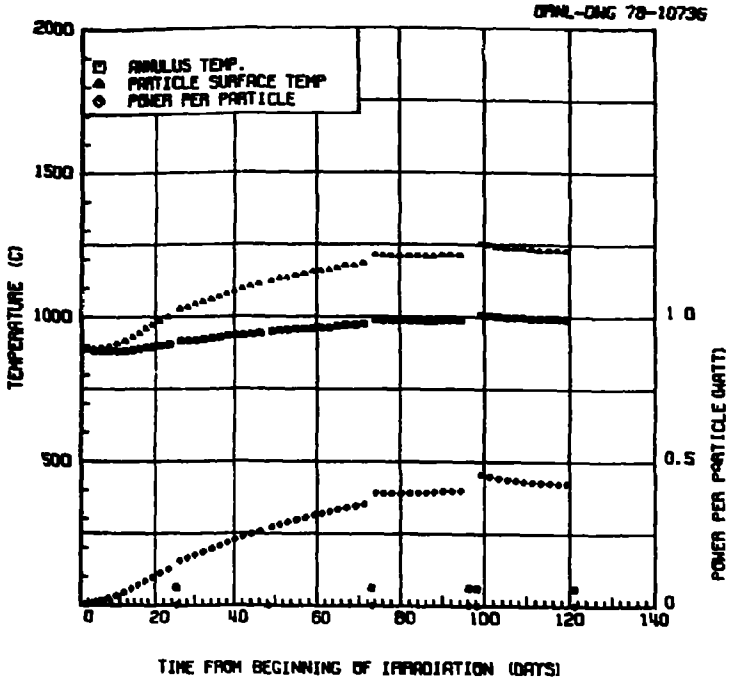

Particle Holder 48, Batch A-782

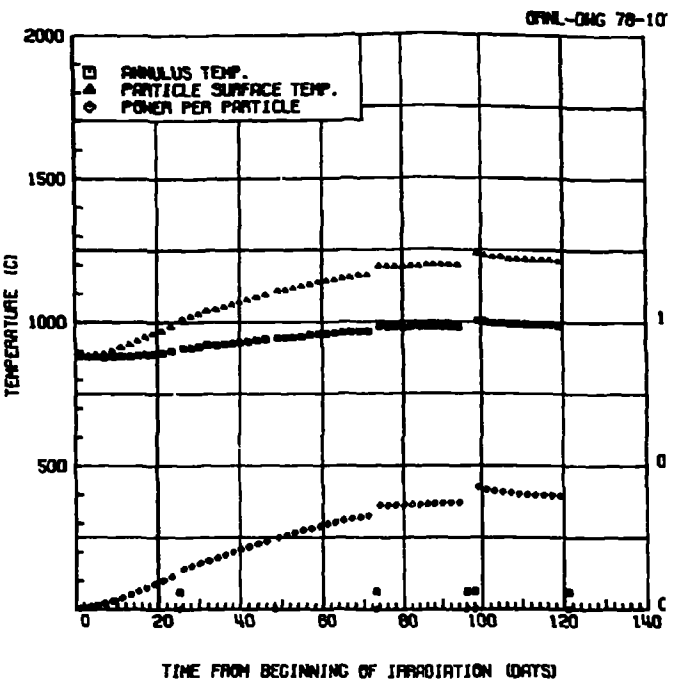

Particle Holder 49, Batch A-786

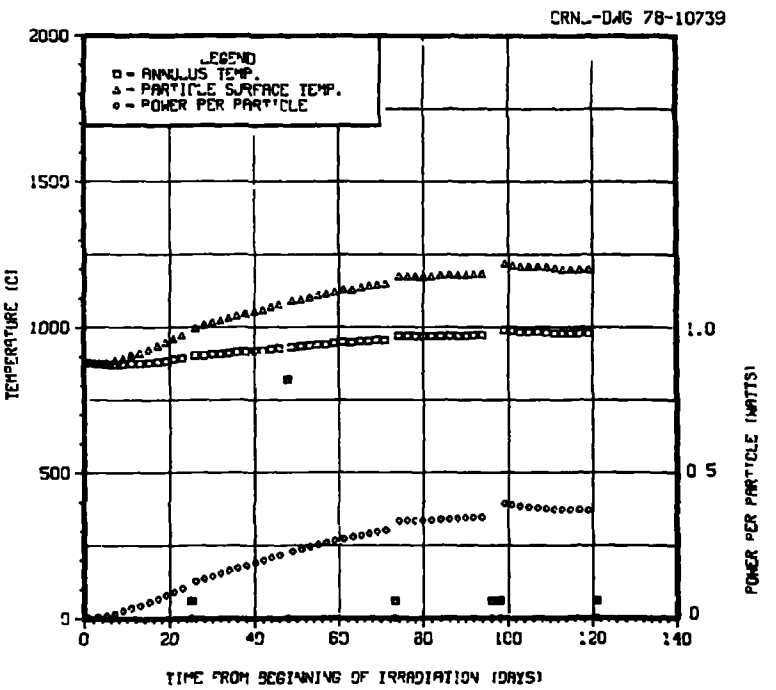

Particle Holder 51, Batch A-787

Fig. A4. Temperature and Power Histories for ORNL Low Temperature Posi

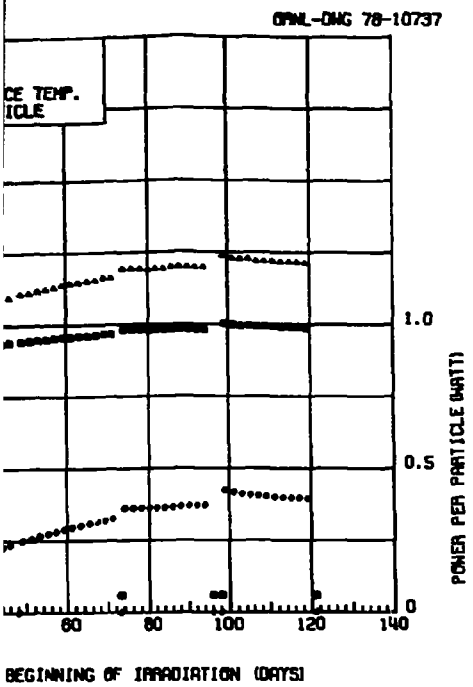

Holder 49, Batch A-786

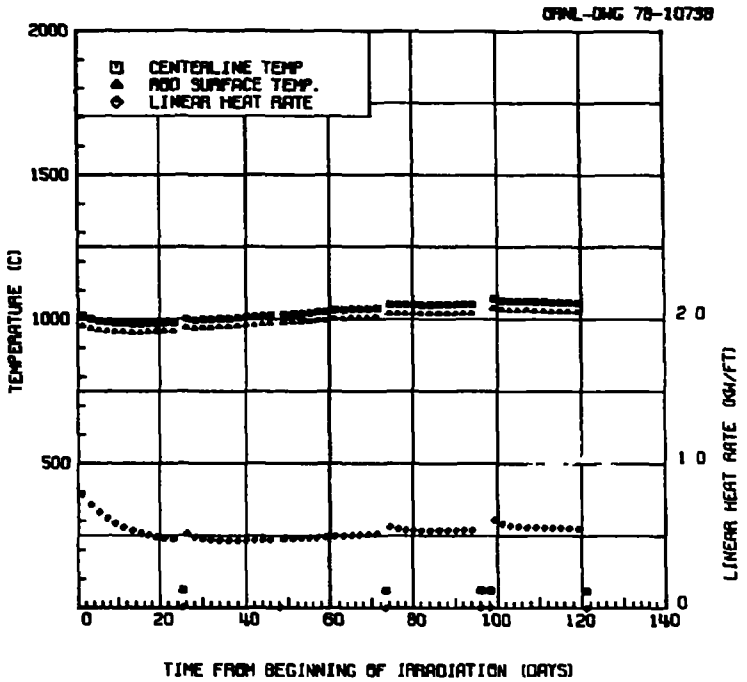

Fuel Rod Number 50, Batch A836+OR2576H

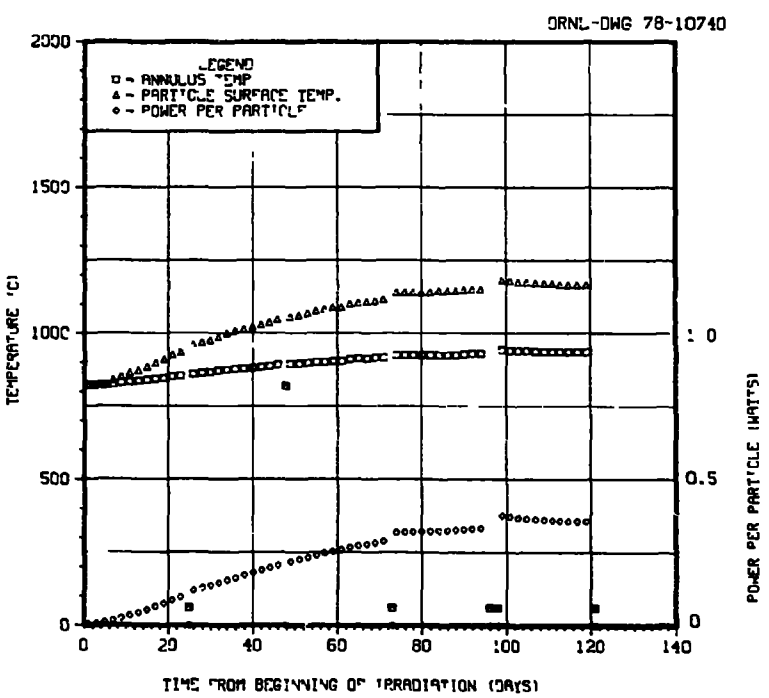

Particle Holder 52, Batch OR-1975-T

ORNL Low Temperature Positions During Irradiation in Capsule HT-34.

APPENDIX B

DIMENSIONAL CHANGES OF INTERNAL COMPONENTS OF CAPSULE HT-34

Appendix B

Dimensional Inspection

The fuel rods, graphite holders, and graphite magazines from HT-34 were measured after irradiation, and the dimensions were compared with the preirradiation values. The resultant changes vs fast fluence for the graphite holders and magazines are shown in Figs. B1 and B2, respectively. Data from previous HT capsules are shown for comparison. The HT-34 fuel rod dimensional data are not shown because we learned later that a knife-edge anvil was used on the dial indicator rather than the usual flat anvil. The knife-edge anvil resulted in what appeared to be unreasonable shrinkage rates, as one would suspect when a sharp edge is pressed onto the porous matrix structure of the fuel rods. The quality assurance procedure for dimensional inspection has been modified to guard against reoccurrence of this problem. Fortunately, sufficient data for fuel rods have been collected from earlier HT capsule experiments that were used in the HT-34 thermal analyses, as shown in Fig. B3.

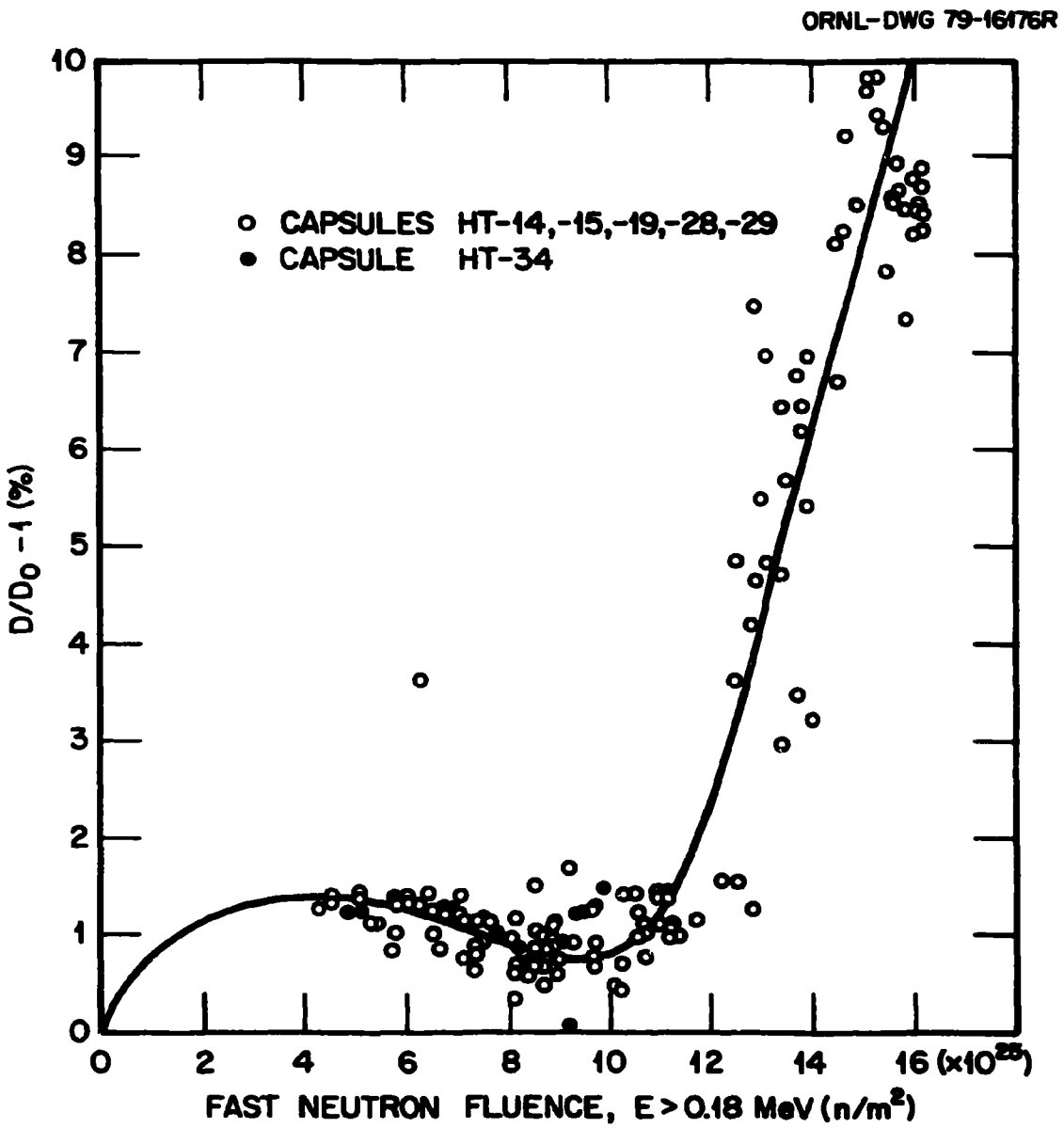

Fig. B1. Correlation of Dimensional Change of POCO Graphite Holders with Fast Neutron Fluence.

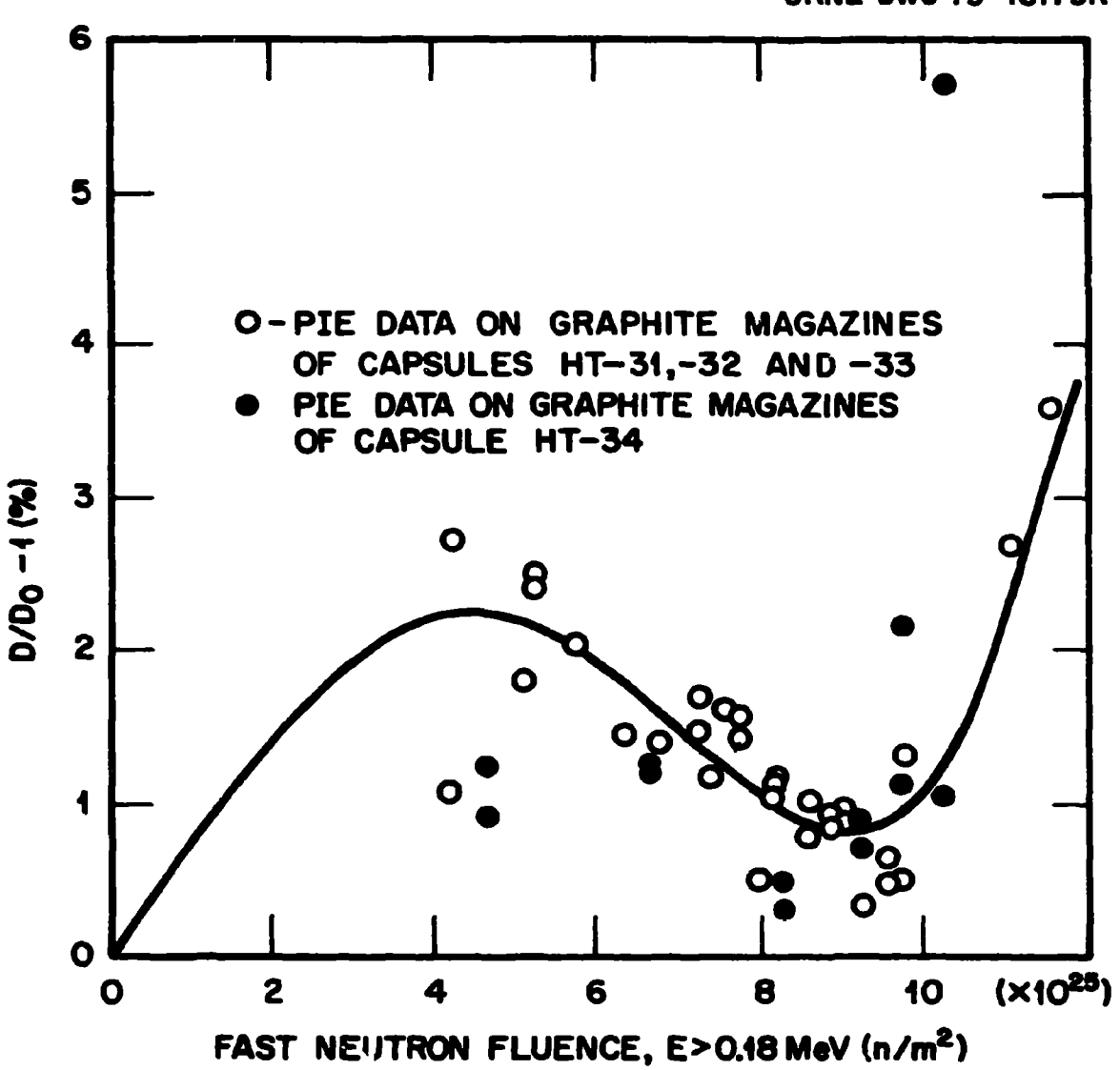

Fig. B2. Changes vs Fast Fluence for Graphite Holders and Magazines.

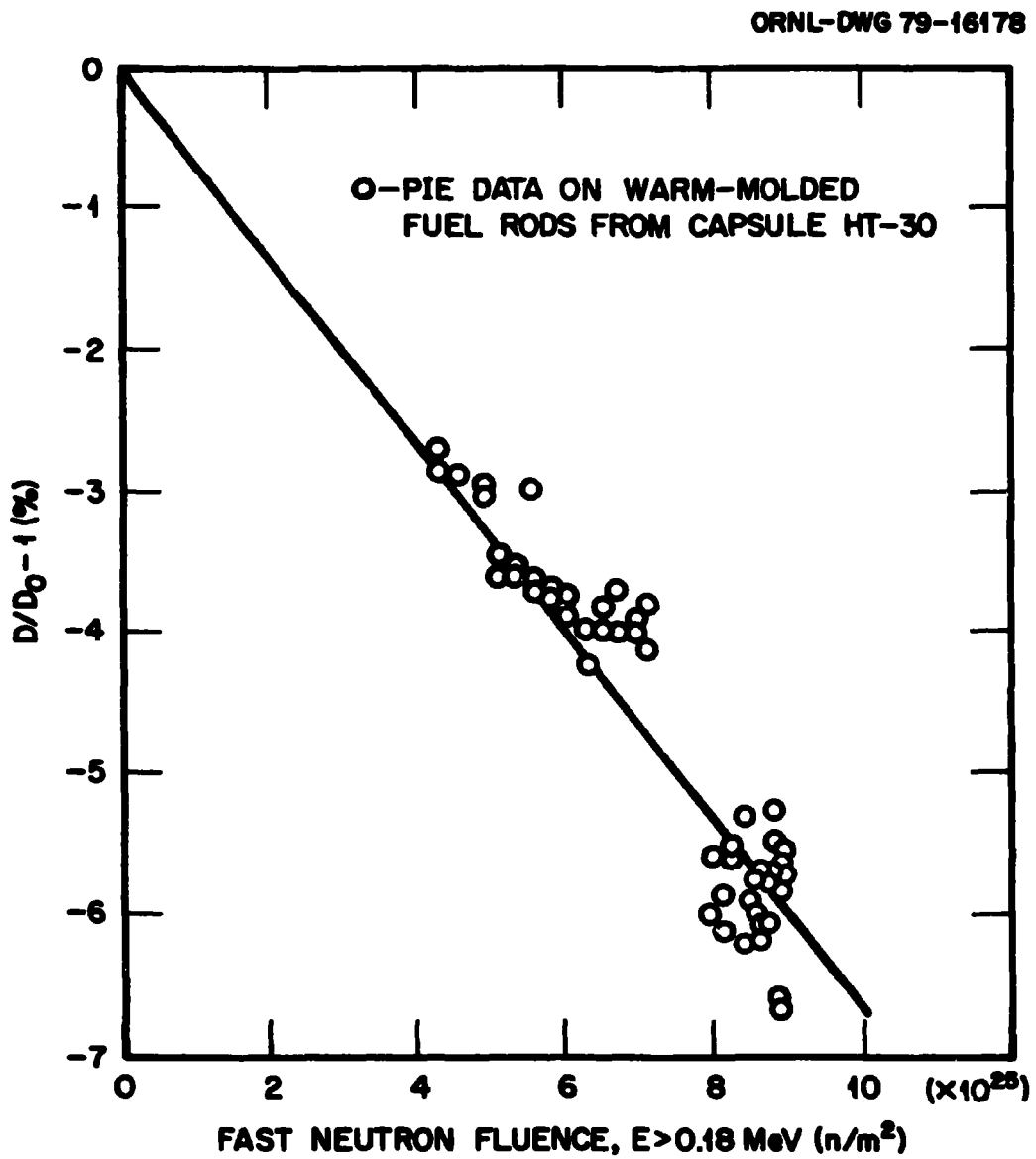

Fig. B3. Irradiation-Induced Shrinkage of Warm-Molded Fuel Rods Irradiated in Capsule HT-30.